Science Advances
AAAS

Supplementary Materials for

Impacts of wind power on air quality, premature mortality, and exposure disparities in the United States

Minghao Qiu *et al.*

Corresponding author: Minghao Qiu, mhqiu@stanford.edu; Noelle E. Selin, selin@mit.edu

Sci. Adv. **8**, eabn8762 (2022)
DOI: 10.1126/sciadv.abn8762

This PDF file includes:

Supplementary Methods

Alternative specifications of the statistical model

Our main specification uses year × month-of-year × hour-of-day fixed effects and only includes total system demand (lagged for up to 24 hours) as the control variables. The time fixed effects control for the long-term, seasonal, as well as the diurnal unobserved effects in wind power and EGU emissions. Our main specification constrains the "diurnal effect" to be constant across all days in the same month, which may not be the case as these patterns could differ between weekdays and weekends or differ on specific dates. To address this issue, we estimate the equations with two other specifications for time fixed effects: (1) year × month-of-year × hour-of-day × day-of-week and (2) year × month-of-year × hour-of-day + year × month-of-year × day-of-month. Specification (1) allows the diurnal effect to differ by day-of-week, and specification (2) incorporates potential differences between different days in the same month. We find the aggregated marginal effects remain highly consistent across different specifications of time fixed effects (results shown in column (2) and (3) of table S1 to S3).

Our main specification does not explicitly capture the potential joint effect of wind power and gas price on coal power plants (*40*).To test the magnitude of this effect, we conduct a sensitivity analysis that includes natural gas prices and the interaction term between gas price and the contemporary wind power in the regression. We use the monthly natural gas price (electric sector) at state level from the EIA-923 reports. The results (coefficients for the main terms of wind power) can be found in column (4) of table S1 to S3. In summary, we find that the marginal effects remain largely similar across models with/without the gas price terms in most ISO regions. The effects of wind power alone on SO_2 emissions increase by 30% (i.e. the emission reductions due to wind power are overestimated when the joint effect of gas prices is not considered) in ERCOT and PJM, consistent with findings from (*40*) that natural gas price and wind power jointly displaces generation from coal. Because quantifying this interaction is not the primary focus of our paper, we still use the original model specification (which focuses on the average impacts) for air quality analysis.

We also include congestion status of the grid as additional control variables. We focus on ERCOT, MISO, NYISO, and PJM, due to the availability of congestion data and the importance of congestion issues (information derived from the recent National Electric Transmission Congestion Study (*74*)). For ERCOT and MISO, we use the constructed hourly dummy variables of the

congestion status (based on zonal congestion prices) from (*41*). For PJM and NYISO, we use the hourly congestion prices (or shadow prices of transmission constraints) as a proxy for the congestion status. The results can be found in column (7) of table S1 to S3. In summary, we find the aggregated marginal effects remain highly similar before/after considering the congestion status in most ISO regions. Only in ERCOT, we observe that the magnitude of SO_2 and NO_x emission reductions increases by ∼10% after controlling for the congestion status. This is consistent with the likely fact that wind power contributes to the transmission congestion, and congestion results in smaller emission offsets from wind power (*41*).

Our main specification uses all non-missing values (including both zeros and non-zeros) of emission and generation at EGU level to estimate the impacts of wind power. This does not differentiate operating hours from non-operating hours in estimating effects of wind power on emissions. In practice, impacts of wind power may be different for operating and non-operating EGUs, as EGUs (coal-fired units in particular) do not usually run at very low capacity factors. To examine the importance of this effect, we evaluate two alternative specifications of our model. In one specification, we re-estimate the impacts of wind power on emissions, solely focusing on the hours that the EGU was in operation (i.e. estimating the regressions only with positive generation and emission values). The results are shown in column (5) in tables S1 to S3). In another specification, we include all operating and non-operating hours in our estimations, and in particular, include all missing values and treat them as zeros. We include all the missing values because missing values may potentially indicate the non-operating status for EGUs. Result of this specification is shown as column (6) in tables S1 to S3). In summary, we find that the marginal effects of wind power on electricity generation and emissions remain largely similar across models regardless of our choices in handling zero values or missing values (except for in ISONE and NYISO where the uncertainty of the estimates are large, and SO_2 emissions for PJM where bituminous coal EGUs are more prevalent).

Changes in electricity export to neighboring regions due to wind power

Our statistical model does not capture the potential effects of wind power on fossil fuel EGUs in the neighboring ISO regions through inter-regional export of electricity. However, increases in wind power can increase the export of electricity generation to the neighboring regions (or decrease import from neighboring regions), and likely displace electricity generation from fossil fuel EGUs in the neighboring regions. For simplicity, we will refer *increases in export* or *decreases in import* as *increases in net export* in this section. Increases in net export of electricity generation due to wind

power provide an upper bound for the potential impacts of wind power on the electricity generation of fossil fuel EGUs in the neighboring regions, since electricity generation from other fuel types can be displaced as well. Following methods from (*10*), we quantify changes in electricity export to neighboring ISO regions due to wind power with the following equation:

$$Y_{i,ymdh} = \beta_i W_{i,ymdh} + \gamma_i X_{i,ymdh} + \delta_{i,ymd} + \eta_{i,h} + \varepsilon_{i,ymdh} \quad [1]$$

where $Y_{i,ymdh}$ is the hourly net export of electricity from ISO i to all neighboring regions at year y, month of year m, day of month d, and hour of day h. $W_{i,ymdh}$ is the wind power production in ISO region i. $X_{i,ymdh}$ is the set of control variables including the solar generation, electricity demand of ISO i, electricity demand, wind and solar generation in all the neighboring regions. $\delta_{i,ymd}$ is the year-month-day fixed effects, and $\eta_{i,h}$ is the hour-of-day fixed effects. β_i is the coefficient of interest that quantifies the increases in electricity net export due to an increase of wind power by 1 MWh. Table S6 shows the estimated increases in electricity export in each ISO region. Estimations are performed with a separate dataset of hourly electricity generation and export from EIA (*39*), which only includes observations starting since July, 2018.

For an increase in wind power by 1 MWh, we estimate that the electricity net export to neighboring regions increases by 0.427 MWh in CAISO, and 0.396 MWh in NYISO. Increases in electricity net export are less substantial in other ISO regions, with an increase by 0.131 MWh in PJM, 0.130 MWh in SPP, 0.122 MWh in MISO, and 0.028 MWh in ERCOT. Quantifying the implications of the increased electricity export on emissions and air quality is challenging because 1) many "neighboring regions" are not in our sample (not ISO regions), 2) the estimation is performed with a different sample during a different time period, and 3) it is difficult to estimate the effects on each individual EGU. Therefore, we only use the estimates from our main model (which only estimates effects within ISO region) in the subsequent analysis on emissions, air quality, and exposure disparities.

Due to the large changes in electricity export in CAISO and NYISO, we perform a sensitivity analysis to quantify the potential effects of the electricity exchange on emissions and air quality in these two regions. In addition to results shown in table S6, we further quantify the changes in electricity exchange with the specific neighboring region due to wind power in CAISO and NYISO. To do this, we re-estimate equation 1 to regress wind power in NYISO or CAISO on its neet export to a specific neighboring region, while controlling for the export to other neighboring regions. Results are shown in table S7. For NYISO, we estimate that 28% and 30% of the wind-driven changes of

electricity exchange is associated with PJM and ISONE (with the rest to Canada). For CAISO, we estimate that 80% and 17% of the wind-driven changes of electricity exchange is associated with the Northwest and Southwest electricity regions, respectively (with the rest to Mexico). We then quantify the effects of the changes of electricity exchange on EGU emissions in ISONE, PJM, Northwest, and Southwest. For ISONE and PJM, we use the EGU-level effects derived from our analysis. For Northwest and Southwest (which are not included in our main analysis), we assume the emissions offset is proportional to the size of fossil EGUs. We then use the InMAP model to estimate the changes in annual $PM_{2.5}$ concentrations due to the increased electricity export (proportional to RPS-related wind power) from NYISO and CAISO. We find that changes in annual $PM_{2.5}$ concentration due to the wind-driven changes of electricity export are ∼7% of the effects of RPS-related wind power estimated in our main analysis (which ignores the electricity export), while most changes occur near a few coal plants in Utah (out of our range of primary analysis). The effects are limited because 1) the amount of wind power in NYISO is quite small, and 2) the electricity grid in the Northwest is quite clean.

Seasonal and diurnal heterogeneity of the marginal effects

In our main analysis, we do not explicitly account for the potentially different marginal impacts of wind power on EGU emissions during different seasons and different hours of the day. To examine the potential importance of this issue, we perform a sensitivity analysis to estimate the impacts of wind power on each individual EGU for different seasons and different hours of the day. To do this, we run the same regression as in the main analysis, but only using data from certain seasons or hours of the day. The results are shown in figure S3 and S4. We find that the effects of wind power on total emissions do not differ substantially across different seasons and hours of the day. For MISO, SPP, PJM and ERCOT (i.e. regions that drive the results of air quality effects), the differences between marginal effects are generally within 16% across different seasons, and within 15% across different hours of the day. The marginal effects of wind power on SO_2 emissions differ by 39% and 29% across different seasons in ERCOT and PJM, respectively. However, these seasonal variations of the emission responses to wind power would still be dominated by the seasonal and diurnal pattern of wind power production itself (which has seasonal and diurnal differences up to 300%).

Examining exposure disparities for different population groups

Environmental justice is a multi-faceted concept, and metrics that apply certain thresholds may not capture the full effects of a policy on the disadvantage communities. As there are varying definitions of EJ, we choose to apply two major criteria drawn from the U.S. EPA's environmental justice screening tool for our primary evaluation of the current distribution of air quality benefits against EJ-relevant targets. To explore additional multi-dimensional aspects of our EJ analysis, we conduct additional analyses to quantify the impacts on many alternative demographic groups.

For analysis on income groups, we quantify the relative benefits of each income group (10 groups in total, from households earning less than 10k annually to those earning over 200k). Doing this allows us to get a more complete understanding of the impacts of wind power development on the pollution disparity by income groups. Results are shown in figure S14 and S17. In general, we find limited differential effects of wind power benefits across different income groups. Population groups with annual household income >200k each year generally get smaller $PM_{2.5}$ benefits (by ~5%) across most states. Groups with household income from 10-75k receive slightly larger benefits (by ~2%). We further quantify the fraction of health benefits accrue to each income group (figure S24).

For analysis on racial/ethnic groups, we quantify the relative benefits for each racial/ethnic group (Black, Hispanic, White, Asian, and Native American), and the fraction of benefits that accrue to each group (shown in figure S14 and S24).

For analysis on groups with different baseline exposure to air pollution, we follow the approach from (*75*) to differentiate grid cells into 10 decile groups based on baseline $PM_{2.5}$ concentration in 2014. We then quantify how wind power influences the air quality in each of the ten groups. This offers us a more complete understanding of the effects of wind power on the existing $PM_{2.5}$ disparities between locations with different baseline pollution conditions. As shown by figure S16 and S18, only the 10-20% dirtiest regions in each state receive larger-than-average benefits (by 5-10%). The cleaner half of each state generally gets lower benefits, with large state-level heterogeneity.

Air quality modeling

We estimate the unit-level impacts of wind power production on air quality using the adjoint of the GEOS-Chem model. We use archived model outputs from Dedoussi et al. (*38*) that calculate the sensitivities of the state-level population-weighted $PM_{2.5}$ and O_3 concentrations to the SO_2 and NO_x emissions changes in each grid cell in the contiguous US. The GEOS-Chem adjoint model is

simulated for the year 2011 with a horizontal resolution of 0.5°×0.666°. EGUs are linked to the location specific sensitivities derived from the adjoint model based on their latitude, longitude and stack height. The marginal impact of wind power on air quality at the EGU level is then calculated as the linear combination of the product of marginal impact of wind power on emissions and the associated air quality sensitivities for both SO_2 and NO_x emissions. In general, the combined sensitivities of SO_2 and NO_x overestimate the impacts of the combined emission changes on air quality due to nonlinear interactions between emitted chemicals (*38*). This effect is likely to be limited here, however, as the marginal emissions changes due to wind power are very small.

To compare with previous studies, we also quantify the air quality impacts with four reduced complexity methods: the InMAP model (*72*), the AP2 model (*76*), the Estimating Air pollution Social Impact Using Regression (EASIUR) model (*77*), and health benefits estimates (per ton of SO_2 and NO_x emissions) developed by the US EPA (*78*) (see figure S8).

We use the GEOS-Chem forward model to simulate the air quality impacts of the wind power used to meet RPS targets in 2014, under different scenarios, and for our analysis of the exposure disparities. We use GEOS-Chem version 12.3.0 with a horizontal resolution of 0.5°× 0.625° in North America. For each forward run, we first simulate a global run at a horizontal resolution of 4°× 5° from January 2014 to December 2014, with a six-month spin-up. These global simulations are then used as the boundary conditions for nested simulations in the US with finer resolution of 0.5°×0.625°. We use meteorological data from the Modern-Era Retrospective analysis for Research and Applications, Version 2 (MERRA 2) (*79*). We use the hourly SO_2 and NO_x emissions reported in AMPD in 2014 as our baseline emissions for the power sector. We add the unit-hour level emissions changes of SO_2 and NO_x due to wind power to the baseline emissions to project the counterfactual emissions in 2014 in absence of this wind power. The emissions of other sectors and other species (NH_3, BC, OC and VOCs) from the power sector are derived from the National Emission Inventory (NEI) of 2011 and are scaled to match the total emissions reported in NEI 2014.

Idealized theoretical scenarios

We design four theoretical scenarios: three that use unit-level emissions intensity (CO_2, SO_2, and NO_x), and one that uses unit-level impacts on premature mortality as the decision criteria. The three emissions minimizing scenarios minimize the total emissions from fossil EGUs and thus maximize the avoided emissions due to wind power generation by displacing electricity generation from EGUs with higher emissions intensity. The health damage minimizing scenario minimizes the health damages

from fossil EGUs based on their impacts on premature mortality.

Our main scenarios do not include any dispatch constraints on how much generation could be displaced for each unit (as long as displacement is below generation for each hour). Therefore, these scenarios are used to provide theoretical (rather than realistic) maxima for emissions reductions and health benefits. We perform sensitivity analyses that evaluate these four scenarios with some dispatch constraints that the electricity generation is allowed to be displaced up to a certain fraction (ranging from 1% to 30%, calculated with the interannual variability of unit-level generation). The extra avoided emissions under the idealized theoretical scenarios (compared with the *ex post* scenario) are 48-65% smaller with the dispatch constraints, but the extra benefits remain substantial (see figure S27). The four main theoretical scenarios displace the same amount of electricity generation as the *ex post* scenario for each ISO region. We also design four additional sensitivity scenarios that displace the same amount of electricity generation as the *ex post* scenario for each state (instead of each ISO region). Scenarios with these alternative constraints are designed to simulate the impacts of a situation in which each state is only allowed to coordinate the dispatch schedule of EGUs within the state to maximize the avoided emissions or health benefits of the renewable policy at the state level (without cross-state coordination).

We also quantify the air quality benefit of wind power development under another counterfactual scenario. In this scenario, we keep the displacement patterns same as the *ex post* scenario, but reallocate the amount of wind power across ISO regions. The amount of wind power is reallocated from ISO regions with low air quality benefits to regions with high air quality benefits. This scenario quantifies the potential air quality effects of alternative siting decisions for wind power deployment (similar ideas have been evaluated for rooftop solar in (*80*)). We focus on the reallocation within ISONE, NYISO, PJM, SPP, and MISO, which are all interconnected as part of the Eastern Interconnection. Following a similar grid stability constraint in Sexton et al., we assume the hypothetical amount of wind power generated to meet RPS targets in one ISO region does not exceed the existing generation associated with RPS by 100%. Reallocating the wind power capacity from ISONE and NYISO to PJM and MISO (where air quality benefits of wind power development are higher) leads to an extra air quality benefit of the same amount of wind power development by 15%.

Supplementary tables

Table S1: Aggregated effects of a marginal increase in wind power (1 MWh) on total electricity generation from fossil fuel EGUs (unit: MWh).

	(1)	(2)	(3)	(4)	(5)	(6)	(7)
CAISO	-0.488	-0.485	-0.675	-0.300	-0.491	-0.587	
	(0.011)	(0.016)	(0.022)	(0.033)	(0.012	(0.015)	
ERCOT	-0.730	-0.701	-1.026	-0.798	-0.730	-0.854	-0.790
	(0.008)	(0.009)	(0.013)	(0.034)	(0.007	(0.013)	(0.009)
ISONE	-0.992	-1.041	-0.938	-0.996	-1.087	-0.891	
	(0.105)	(0.165)	(0.136)	(0.132)	(0.098)	(0.114)	
MISO	-0.884	-0.869	-0.834	-0.918	-0.849	-0.910	-0.879
	(0.013)	(0.016)	(0.017)	(0.022)	(0.011)	(0.018)	(0.016)
NYISO	-0.443	-0.400	-0.339	-0.300	-0.412	-0.346	-0.426
	(0.034)	(0.041)	(0.048)	(0.059)	(0.034)	(0.062)	(0.037)
PJM	-1.097	-1.065	-0.926	-1.269	-1.088	-0.842	-1.079
	(0.036)	(0.042)	(0.043)	(0.053)	(0.032)	(0.057)	(0.037)
SPP	-0.935	-0.911	-1.072	-0.887	-0.951	-0.839	
	(0.010)	(0.013)	(0.015)	(0.024)	(0.010)	(0.015)	
Year × Month × Hour	Y		Y	Y	Y	Y	Y
Year × Month × Hour × Day of week		Y					
Year × Month × Day of Month			Y				
Gas price				Y			
Excluding zeros					Y		
Including NAs						Y	
Congestion status							Y

Notes: Aggregated effects are calculated as the sum of EGU-level effects within each ISO region. Standard errors are reported in parentheses. Standard errors of the aggregate effects are calculated with the EGU-level standard errors, assuming independence between these EGU-level estimates.

Table S2: Aggregated effects of a marginal increase in wind power (1 MWh) on total SO_2 emissions (unit: lbs).

	(1)	(2)	(3)	(4)	(5)	(6)	(7)
CAISO	-0.001	-0.002	-0.001	-0.001	-0.001	-0.001	
	(0.000)	(0.000)	(0.000)	(0.000)	(0.000)	(0.000)	
ERCOT	-0.515	-0.797	-0.489	-0.755	-0.528	-0.441	-0.563
	(0.022)	(0.030)	(0.026)	(0.082)	(0.021)	(0.025)	(0.030)
ISONE	-0.057	-1.084	-0.605	0.083	-0.121	0.328	
	(0.333)	(0.804)	(0.588)	(0.399)	(0.329)	(0.149)	
MISO	-1.053	-1.075	-1.027	-1.075	-1.040	-0.976	-1.128
	(0.042)	(0.039)	(0.051)	(0.061)	(0.042)	(0.044)	(0.057)
NYISO	-0.105	-0.008	-0.156	-0.034	-0.131	-0.030	-0.118
	(0.032)	(0.039)	(0.041)	(0.058)	(0.036)	(0.018)	(0.036)
PJM	-2.215	-1.671	-2.331	-2.987	-2.142	-1.312	-2.192
	(0.212)	(0.223)	(0.257)	(0.410)	(0.233)	(0.245)	(0.241)
SPP	-0.925	-0.779	-0.921	-0.807	-0.934	-0.789	
	(0.020)	(0.024)	(0.027)	(0.043)	(0.021)	(0.026)	
Year × Month × Hour	Y		Y	Y	Y	Y	Y
Year × Month × Hour × Day of week		Y					
Year × Month × Day of Month			Y				
Gas price				Y			
Excluding zeros					Y		
Including NAs						Y	
Congestion status							Y

Notes: Aggregated effects are calculated as the sum of EGU-level effects within each ISO region. Standard errors are reported in parentheses. Standard errors of the aggregate effects are calculated with the EGU-level standard errors, assuming independence between these EGU-level estimates.

Table S3: Aggregated effects of a marginal increase in wind power (1 MWh) on total NO_x emissions (unit: lbs).

	(1)	(2)	(3)	(4)	(5)	(6)	(7)
CAISO	-0.010	-0.008	-0.004	0.011	-0.011	-0.017	
	(0.004)	(0.005)	(0.006)	(0.011)	(0.004)	(0.002)	
ERCOT	-0.194	-0.305	-0.189	-0.113	-0.196	-0.181	-0.241
	(0.005)	(0.008)	(0.006)	(0.020)	(0.005)	(0.006)	(0.013)
ISONE	0.279	0.006	0.298	0.330	0.256	0.083	
	(0.075)	(0.121)	(0.138)	(0.096)	(0.074)	(0.037)	
MISO	-0.611	-0.554	-0.607	-0.609	-0.612	-0.558	-0.622
	(0.015)	(0.019)	(0.018)	(0.026)	(0.015)	(0.016)	(0.018)
NYISO	-0.018	0.001	-0.015	0.012	-0.017	-0.009	-0.015
	(0.011)	(0.015)	(0.013)	(0.021)	(0.011)	(0.010)	(0.012)
PJM	-0.853	-0.702	-0.852	-0.939	-0.850	-0.615	-0.847
	(0.047)	(0.057)	(0.058)	(0.073)	(0.050)	(0.057)	(0.051)
SPP	-0.761	-0.912	-0.751	-0.650	-0.828	-0.571	
	(0.014)	(0.021)	(0.017)	(0.034)	(0.015)	(0.013)	
Year × Month × Hour	Y		Y	Y	Y	Y	Y
Year × Month × Hour × Day of week		Y					
Year × Month × Day of Month			Y				
Gas price				Y			
Excluding zeros					Y		
Including NAs						Y	
Congestion status							Y

Notes: Aggregated effects are calculated as the sum of EGU-level effects within each ISO region. Standard errors are reported in parentheses. Standard errors of the aggregate effects are calculated with the EGU-level standard errors, assuming independence between these EGU-level estimates.

Table S4: Heterogeneous impacts of wind power on EGUs of different characteristics

	Electricity	CO_2	SO_2	NO_x
max heat input	-0.052	-0.056	0.056^{*}	-0.010
	(0.044)	(0.042)	(0.030)	(0.034)
age	-0.107^{**}	-0.103^{**}	-0.018	-0.070
	(0.054)	(0.051)	(0.052)	(0.074)
NO_x removal	-0.375^{*}	-0.405^{*}	-0.335^{**}	-0.087
	(0.222)	(0.207)	(0.149)	(0.173)
SO_2 removal	-0.111	-0.127	-0.147^{**}	-0.182^{*}
	(0.103)	(0.111)	(0.063)	(0.095)
fuel NG	-0.477^{***}	-0.519^{***}	-0.172	-0.311
	(0.172)	(0.178)	(0.149)	(0.197)
fuel SUB	-0.277^{**}	-0.339^{***}	-0.139^{*}	-0.288^{**}
	(0.118)	(0.128)	(0.081)	(0.114)
Observations	1,205	1,186	1,205	1,205
Adjusted R^2	0.158	0.162	0.014	0.041

Notes: Dependent variables (the relative sensitivity of electricity generation and emissions), the maximum capacity of heat input and unit age are normalized. Relative sensitivity is calculated as the fraction of emissions or generation change due to marginal increase of wind power at the EGU level. Standard errors clustered at plant level are reported in parentheses. For fuel type, the reference/omitted category is bituminous coal. Significance: $*$ p<0.10, $**$ p<0.05, $***$ p<0.01

Table S5: Avoided mortalities due to wind power associated with RPS in different scenarios estimated with alternative concentration response functions.

	ex post	health damage minimizing	SO_2 minimizing	NO_x minimizing	CO_2 minimizing
Krewski et al., 2009	231 (146, 318)	1009 (637, 1391)	927 (586, 1278)	701 (443, 967)	496 (313, 684)
Lepeule et al., 2012	355 (287, 843)	2425 (1253, 3679)	2229 (1152, 3382)	1686 (871, 2557)	1193 (616, 1811)
Hoek et al., 2013	247 (166, 326)	1079 (726, 1425)	992 (668, 1310)	750 (505, 990)	531 (357, 701)
Di et al., 2017	299 (291, 306)	1305 (1270, 1339)	1199 (1167, 1231)	907 (883, 931)	642 (625, 659)
Pope et al., 2018	247 (42, 442)	1079 (184, 1932)	992 (169, 1776)	750 (128, 1343)	531 (91, 951)

Notes: We calculate the $PM_{2.5}$-related all-cause avoided mortality due to wind power under different scenarios. The 95% confidence interval is shown in the parenthesis.

Table S6: Changes in electricity export to neighboring regions due to increases in wind power.

	CAISO	ERCOT	ISONE	MISO	NYISO	PJM	SPP
	(1)	(2)	(3)	(4)	(5)	(6)	(7)
Wind	0.427***	0.028***	0.070***	0.122***	0.396***	0.131***	0.130***
	(0.022)	(0.001)	(0.024)	(0.006)	(0.026)	(0.010)	(0.003)
Observations	55,079	55,080	55,080	55,078	55,080	55,079	55,077
R^2	0.815	0.651	0.855	0.879	0.828	0.916	0.755

Notes: This table shows changes in electricity export to neighboring regions due to an increase in wind power for each ISO region (unit: MWh per MWh wind power). The dependent variable is the export of electricity to neighboring regions (positive values indicate net export). The estimations are performed with hourly electricity generation data from EIA-930, from July 2018 to October 2021 (using all available data). Control variables include electricity demand and solar power in the ISO region, and demand, wind power and solar power in the neighboring ISO regions. Standard errors are clustered at year-month-day level.

Table S7: Changes in electricity export to neighboring regions due to increases in wind power (CAISO and NYISO).

	CAISO-NW	CAISO-SW	CAISO-MEX	NYISO-PJM	NYISO-ISONE	NYISO-CAN
	(1)	(2)	(3)	(4)	(5)	(6)
Wind	0.245***	0.060***	0.012***	0.140***	0.154***	0.204***
	(0.016)	(0.012)	(0.001)	(0.016)	(0.017)	(0.019)
Observations	55,079	55,079	55,079	55,080	55,080	55,080
R^2	0.865	0.907	0.745	0.867	0.849	0.755

Notes: This table shows changes in electricity export to each neighboring region due to increases in wind power in CAISO and NYISO (unit: MWh per MWh wind power). The dependent variable is the export of electricity to a specific neighboring region, e.g., from CAISO to Northwest (NW). SW: Southwest; MEX: Mexico; CAN: Canada. The estimations are performed with hourly electricity generation data from EIA-930, from July 2018 to October 2021 (using all available data). Control variables include electricity demand and solar power in the ISO region, and demand, wind power and solar power in the neighboring ISO regions. Standard errors are clustered at year-month-day level.

Supplementary figures

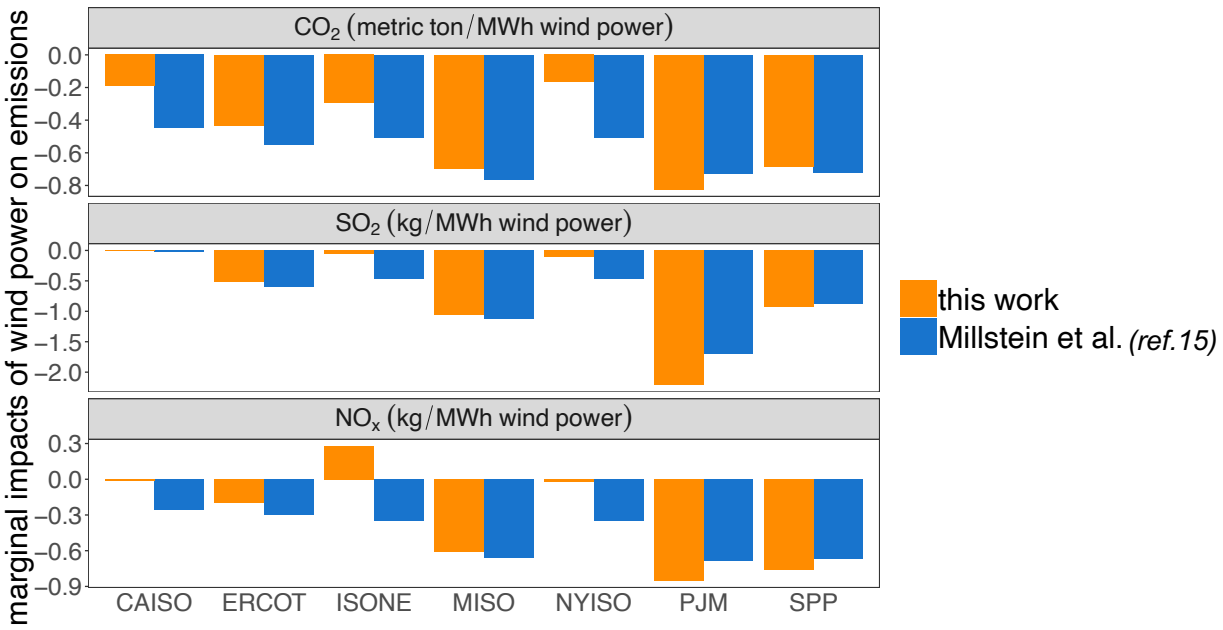

Figure S1: Comparison of the marginal impacts of wind power on CO_2, SO_2, and NO_x emissions estimated in our work (orange) with the estimates reported in Millstein et al. (blue) (ref *15*).

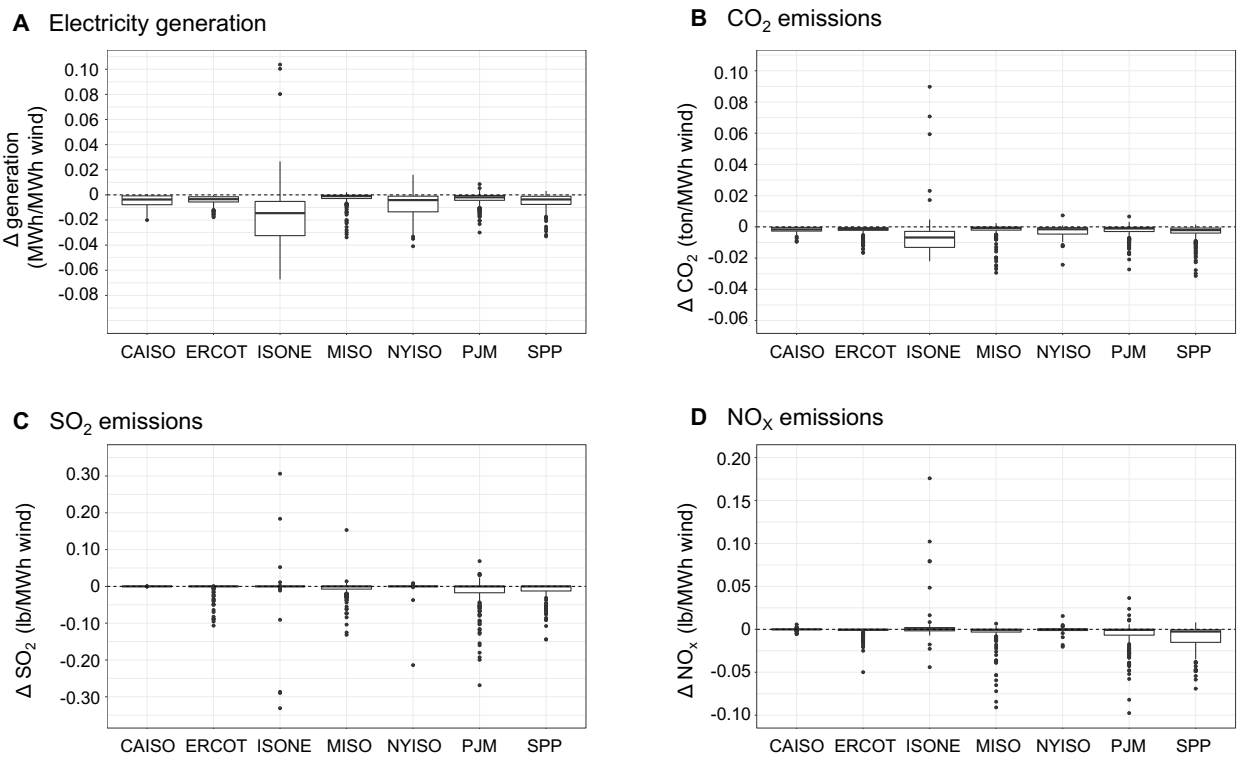

Figure S2: Distribution of the unit-level marginal impacts of wind power on electricity generation (A), CO_2 emissions (B), SO_2 emissions (C), and NO_x emissions (D).

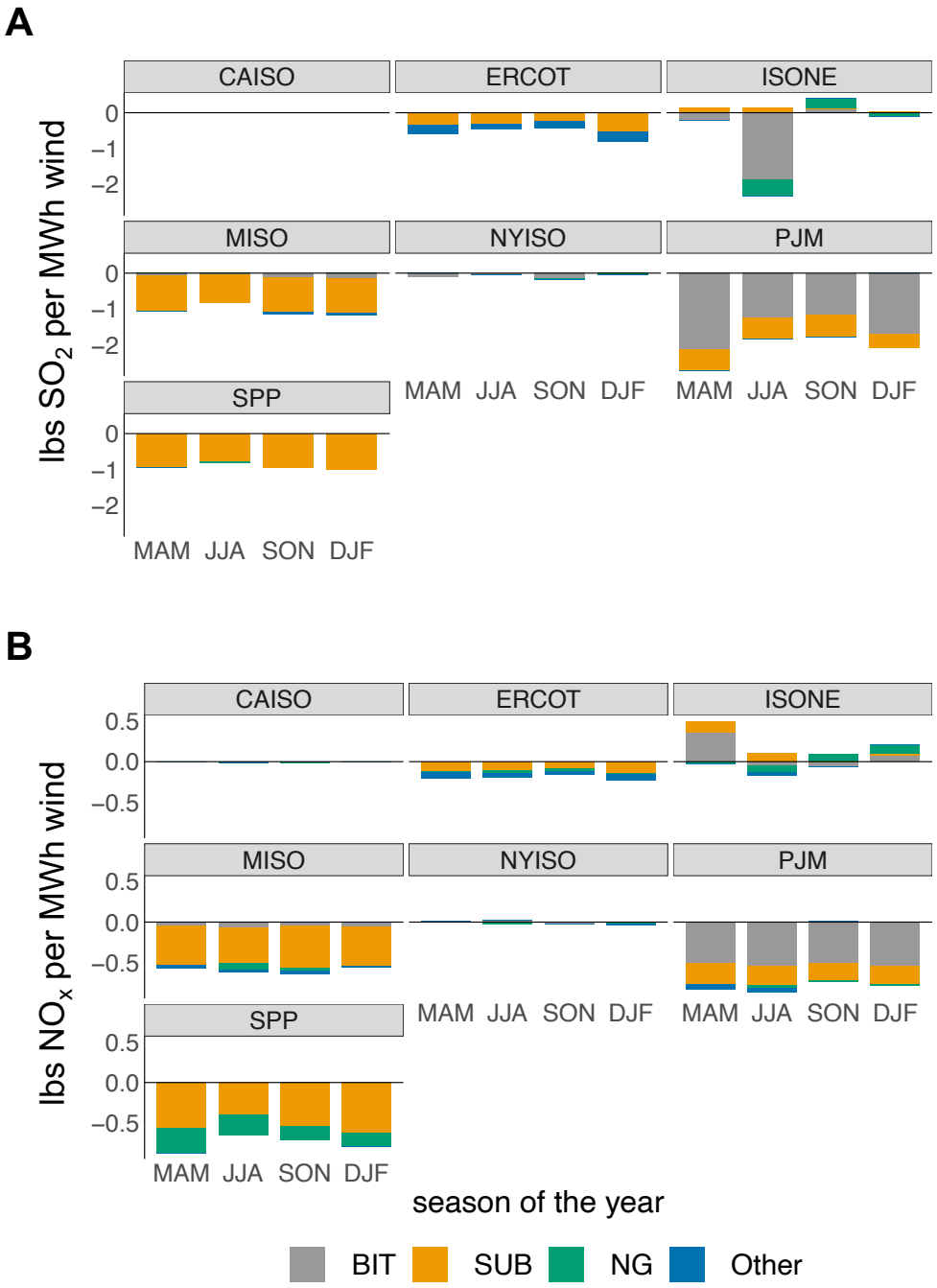

Figure S3: Aggregated impacts of wind power on SO_2 and NO_x emissions within each ISO region, by different seasons. The results are estimated using data in each of the seasons respectively: MAM (March, April, May), JJA (June, July, August), SON (September, October, November), and DJF (December, January, February).

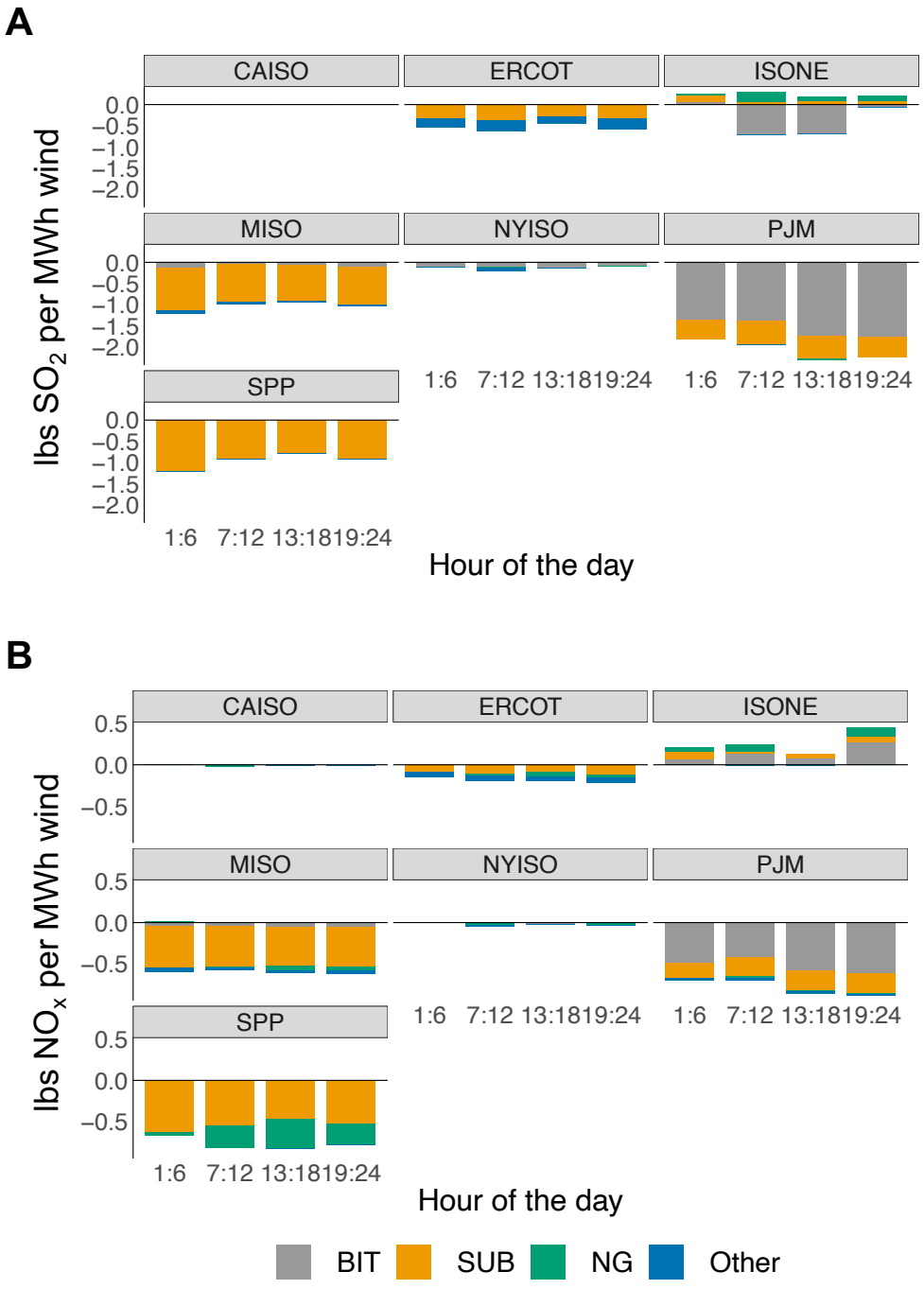

Figure S4: Aggregated impacts of wind power on SO_2 and NO_x emissions within each ISO region, by different hours of the day. The results are estimated using data in each of these periods respectively: 1am-6am, 7am-12pm, 13pm-18pm, 19pm-12am.

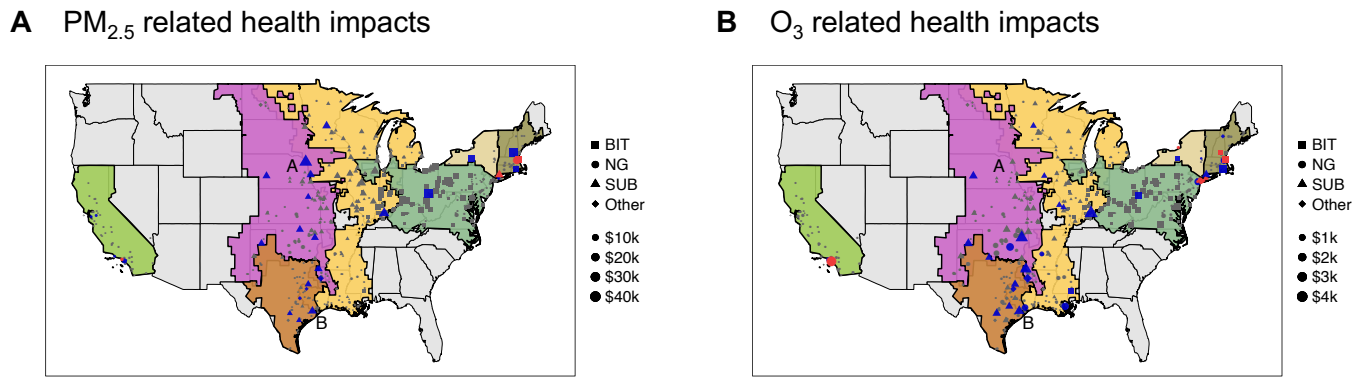

Figure S5: Unit-level impacts of wind power on monetized health impacts due to changes in $PM_{2.5}$ and O_3 concentrations (2014 dollars). Premature mortalities are derived using changes in the annual average $PM_{2.5}$ and MDA8 O_3 across the contiguous US from 1 MWh wind power per hour during the whole year (therefore 24×365 MWh). Health impacts are monetized using a value of statistical life (VSL) of 7.4 million dollars (2006 dollars) recommended by EPA (*44*). Seven ISO regions are colored on the map. Colored plants on the map represent plants whose health impacts account for more than 5% of the total health impacts of all units in the ISO region (only plants with >10% of the total ISO impacts are colored in the ISONE and NYISO regions). Blue indicates health benefits from avoided mortality, while red indicates health damages from increased mortality. Point A and B on the maps show two power plants as illustrations (discussed in the text). We scale VSL value to the 2014 dollars to adjust for inflation. Monetized impacts are expressed in 2014 dollars.

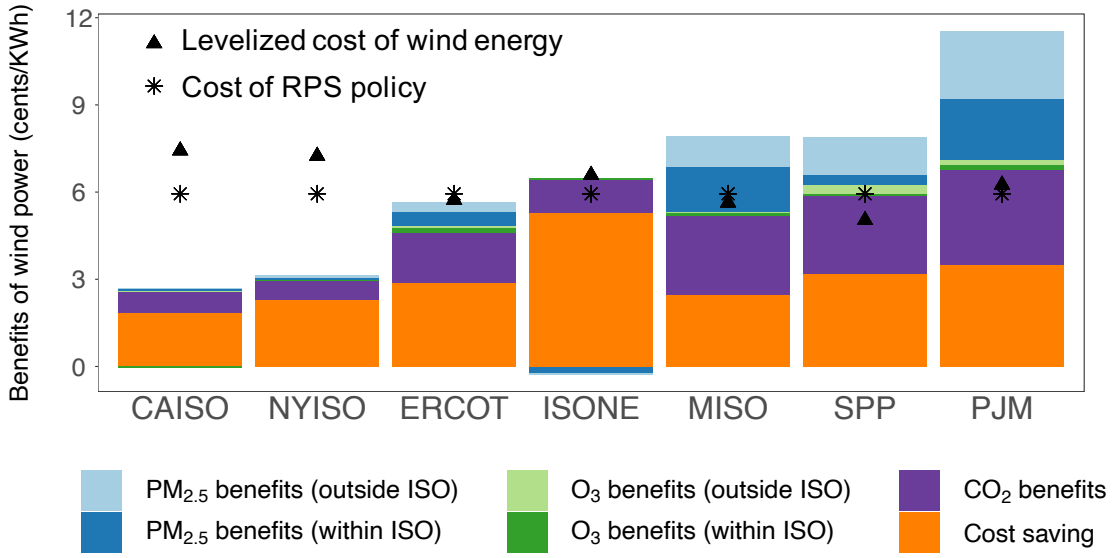

Figure S6: Benefits of wind power from air quality improvements, cost savings and CO_2 reductions at the ISO level (2014 dollars), compared to cost estimates of wind power development. Levelized cost of wind energy is derived from 2017 Cost of Wind Energy Review (*49*) and adjusted for the regional capacity factors of wind energy. Cost of RPS policy represents the loss of household consumption due to the constraints of RPS, derived from Dimanchev et al., 2019 (*19*). Health impacts are monetized using a value of statistical life (VSL) of 7.4 million dollars (year 2006 dollars) recommended by the US EPA. CO_2 benefits are calculated using a social cost of carbon (SCC) of $35 (year 2007 dollars). We scale SCC and VSL values to year 2014 dollars to adjust for inflation. Monetized benefits are expressed in 2014 dollars.

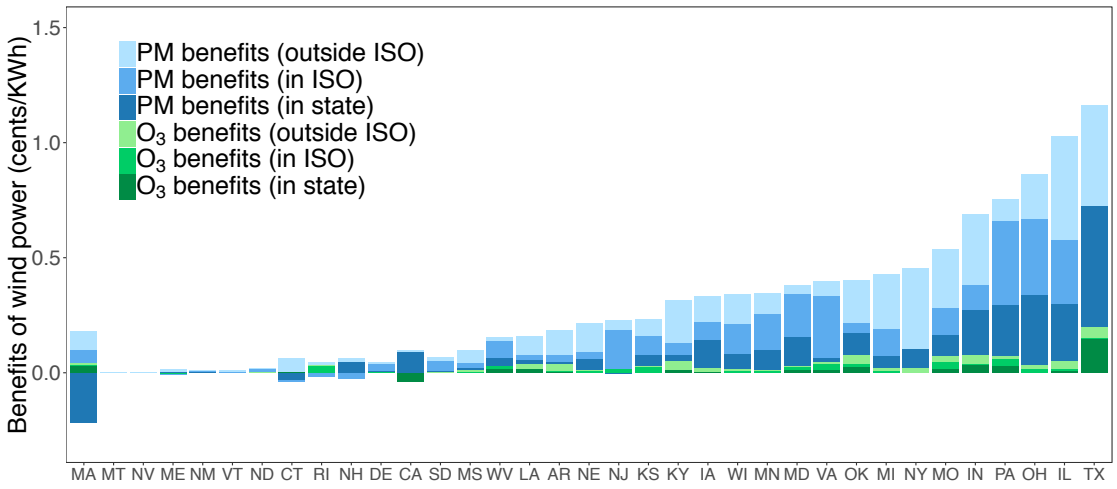

Figure S7: Air quality benefits of wind power at the state level (2014 dollars). Order of the states is based on their total air quality benefits (from left to right, small to large).

Figure S8: Marginal impacts of wind power on the air pollution-related health impacts estimated in our work (orange) and estimates reported in Millstein et al. (blue) (ref *15*). Orange square indicates the estimates reported in our main text (calculated using the GEOS-Chem adjoint model). Other orange dots indicate the impacts calculated with alternative valuation approaches using our estimates of unit-level emissions impacts (see SI section "Air quality modeling"). Blue dots indicate the estimates reported in Millstein et al. under different valuation approaches. For simplicity, we calculate the "EASIUR", "EPA", and "COBRA" estimates by averaging over the high and low estimates of each method reported in Millstein et al. Population and VSL are adjusted to be consistent across different approaches. All estimates are adjusted to dollars in 2014 by scaling VSL values to year 2014 dollars to adjust for inflation.

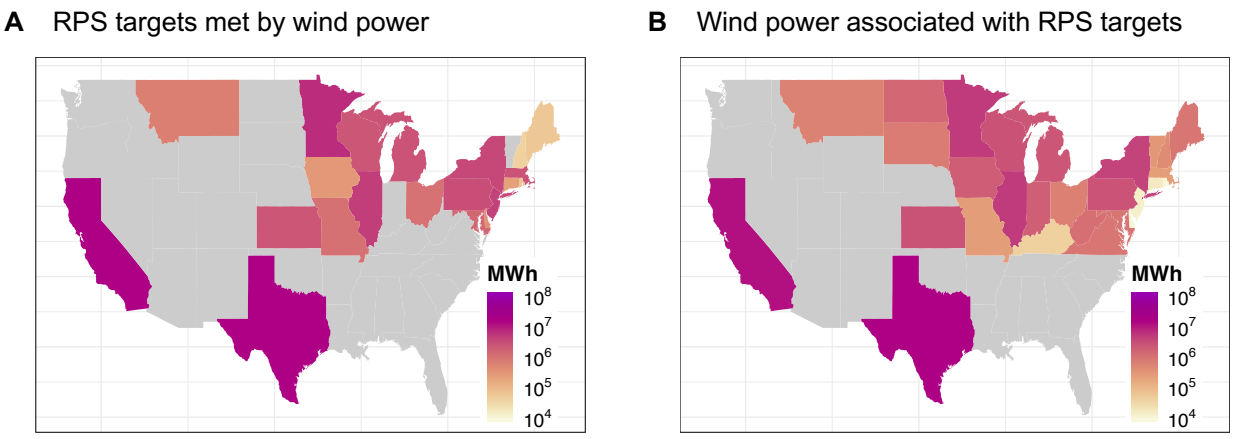

Figure S9: RPS annual targets associated with wind power in 2014.

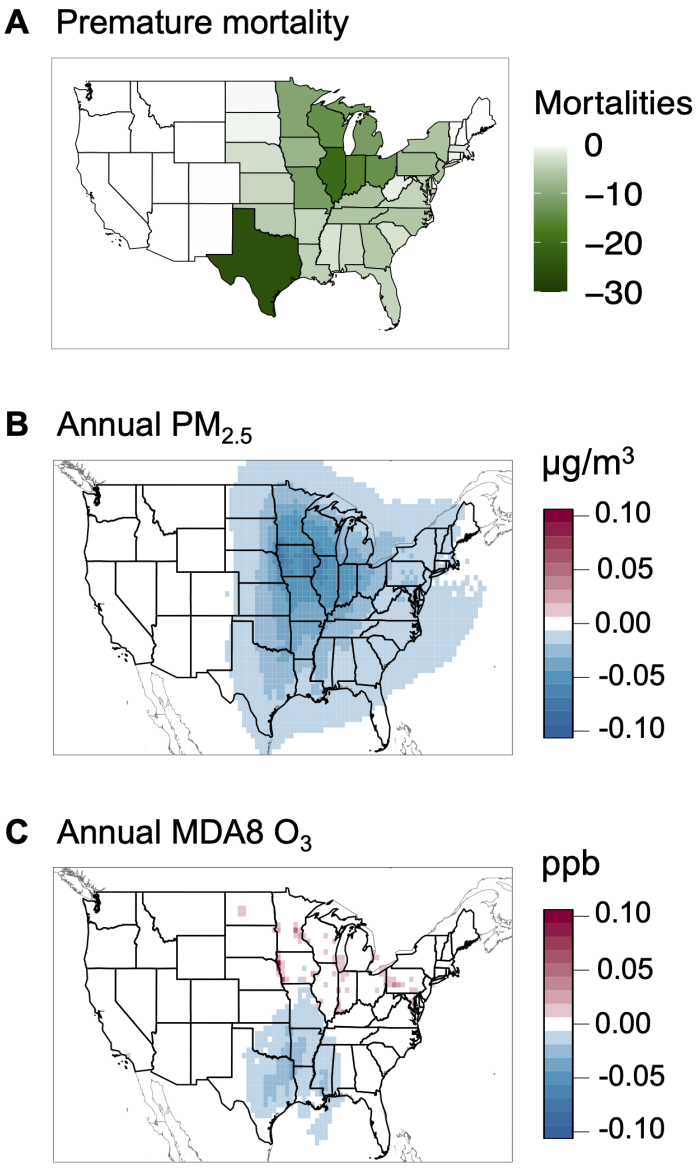

Figure S10: Impacts of wind power used to meet RPS targets on premature mortality, $PM_{2.5}$, and O_3 concentrations under the *ex post* scenario. Premature mortality includes all cause mortality due to $PM_{2.5}$ exposure and O_3 mortality attributed to respiratory diseases. Air quality impacts are characterized as the changes in annual average $PM_{2.5}$ concentrations (unit: $\mu g/m^3$) and the annual average MDA8 O_3 (unit: ppb).

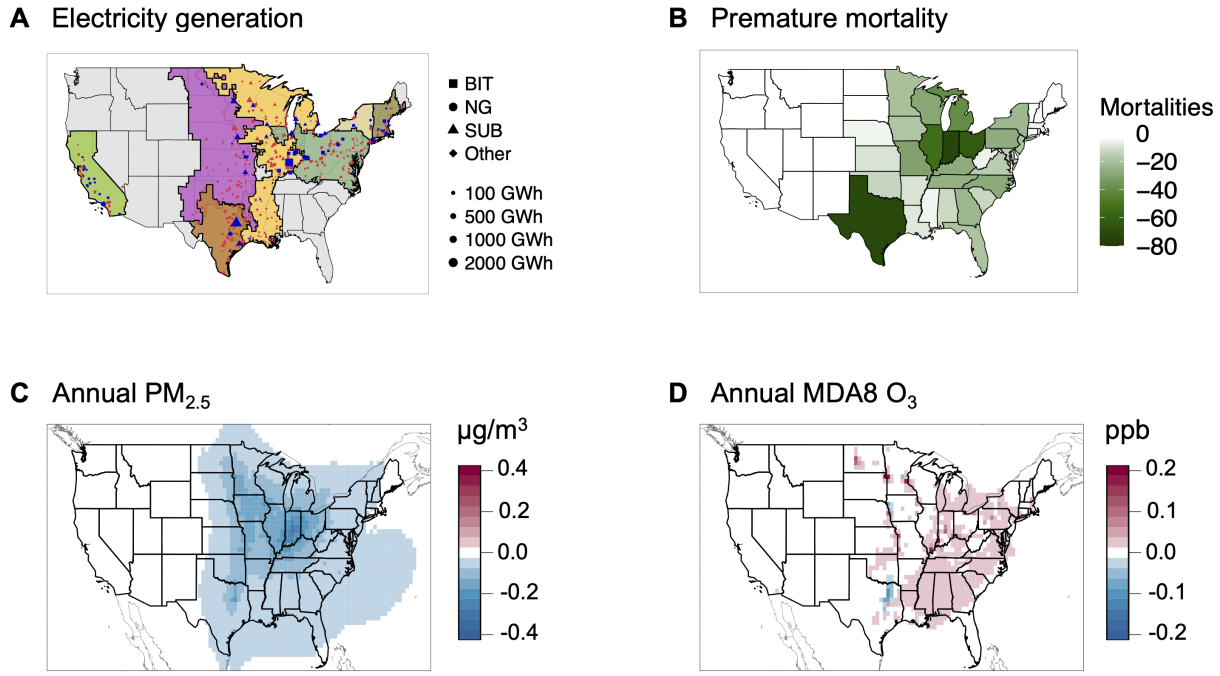

Figure S11: Additional impacts of wind power used to meet RPS targets on electricity generation, premature mortalities, $PM_{2.5}$ and O_3 concentrations under the health damage minimizing scenario relative to the *ex post* scenario. Panel A shows the changes in electricity generation at the EGU level (blue: higher displaced generation due to wind power under the health damage minimizing scenario; red: lower displaced electricity generation). Premature mortality includes all cause mortality due to $PM_{2.5}$ exposure and O_3 mortality attributed to respiratory diseases. Air quality impacts are characterized as the changes in annual average $PM_{2.5}$ concentrations (unit: $\mu g/m^3$) and the annual average MDA8 O_3 (unit: ppb).

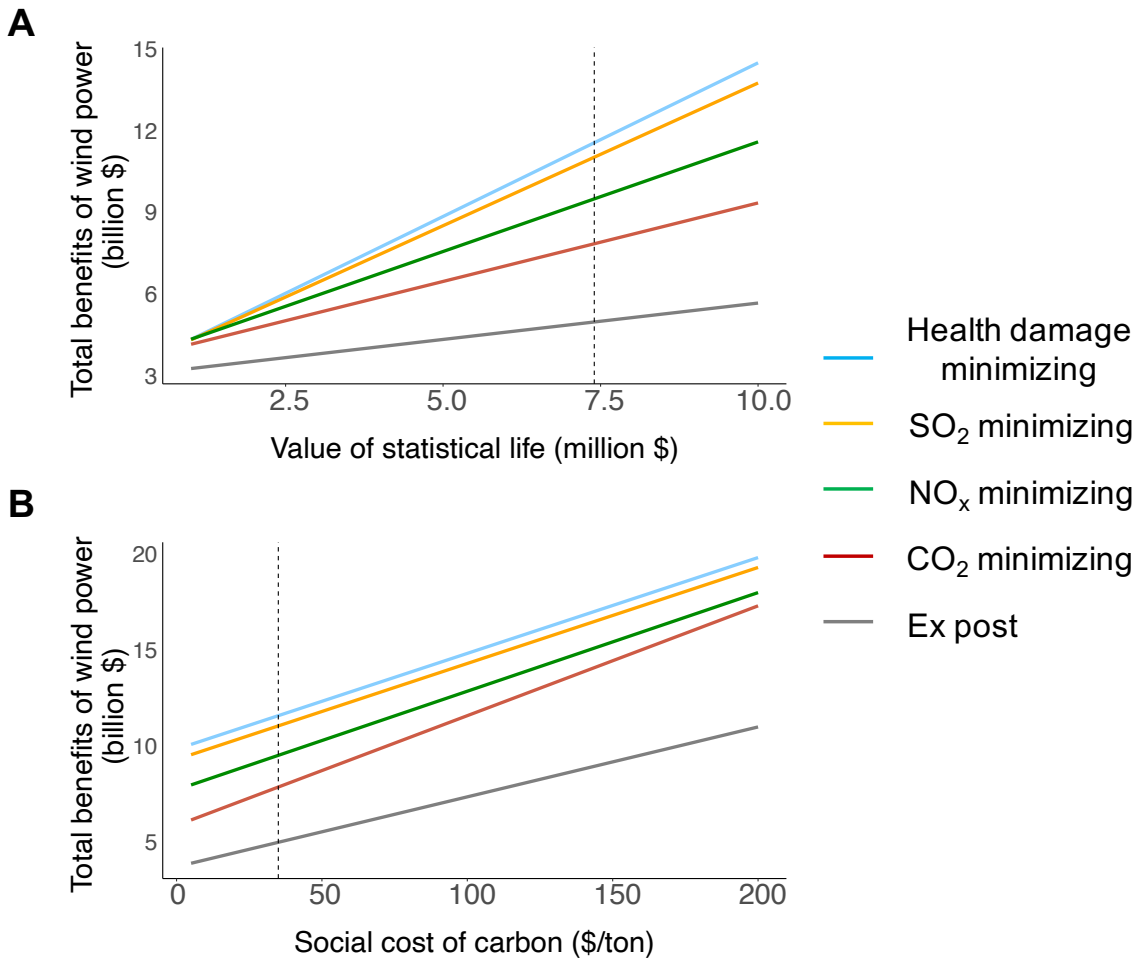

Figure S12: Total benefits of wind power under different scenarios, as functions of value of statistical life (x-axis, panel A) and social cost of carbon (x-axis, panel B). Total benefits are quantified as the sum of health benefits due to reduction in air pollution, climate benefits, and cost saving. The values of VSL and SCC used in the main analysis are shown with the dashed lines. Monetized benefits are expressed in 2014 dollars.

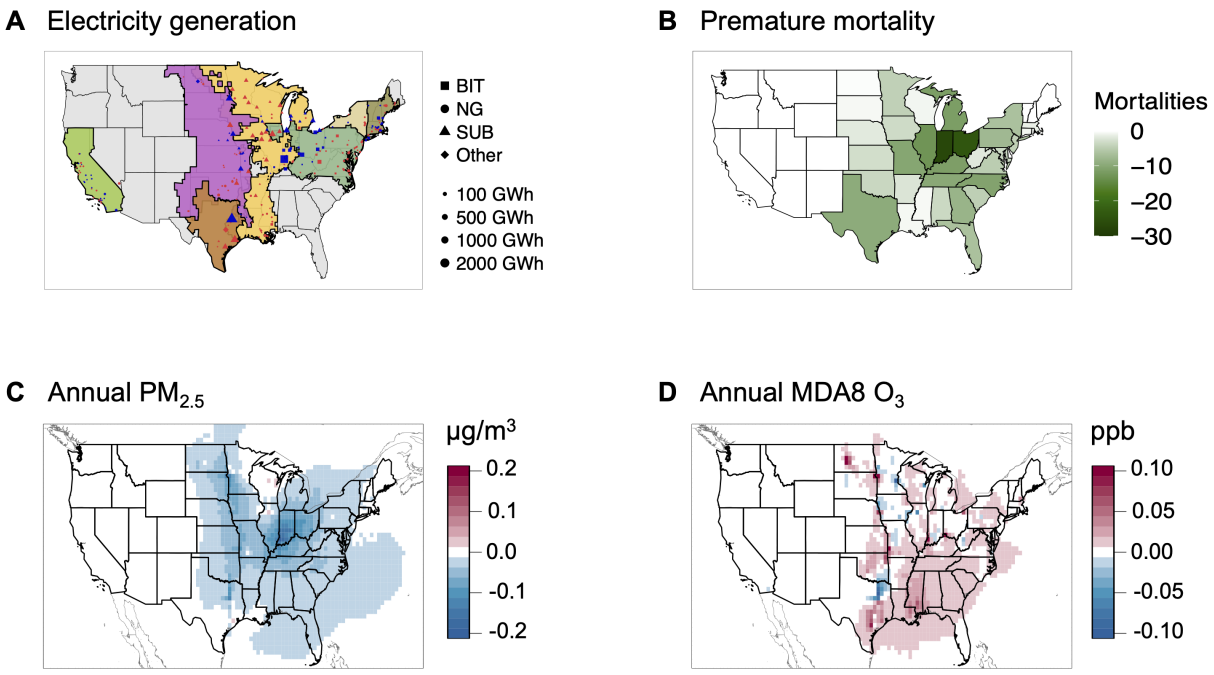

Figure S13: Additional impacts of wind power used to meet RPS targets on electricity generation, premature mortalities, $PM_{2.5}$ and O_3 concentrations under the health damage minimizing scenario relative to the scenario which states make their own decision to minimize health damages (without cross-state cooperation). Panel A shows the changes in electricity generation at the EGU level (blue: higher displaced generation due to wind power under the health damage minimizing scenario; red: lower displaced electricity generation). Premature mortality includes all cause mortality due to $PM_{2.5}$ exposure and O_3 mortality attributed to respiratory diseases. Air quality impacts are characterized as the changes in annual average $PM_{2.5}$ concentrations (unit: $\mu g/m^3$) and the annual average MDA8 O_3 (unit: ppb).

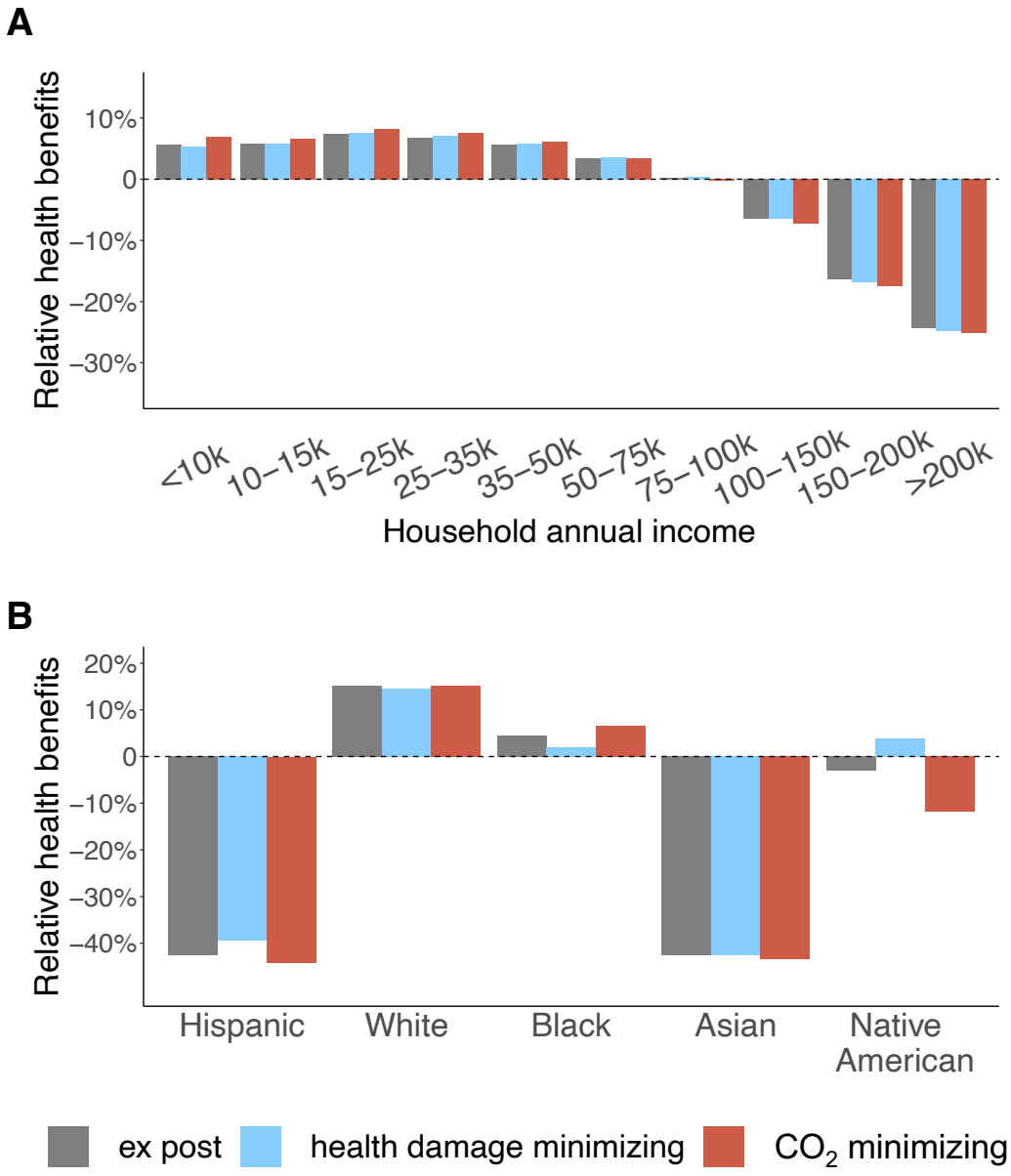

Figure S14: Percentage difference in air quality benefits for different income groups (upper panel) and racial/ethnic groups (lower panel). Benefits are calculated as the relative differences between the mortality rate changes experienced by specific population groups and the nation-wide mortality rate change due to wind power. Positive relative benefits indicate the subgroup experiences a larger reduction in mortality rates compared to the average population in the studied regions. The three emissions scenarios are shown in different colors.

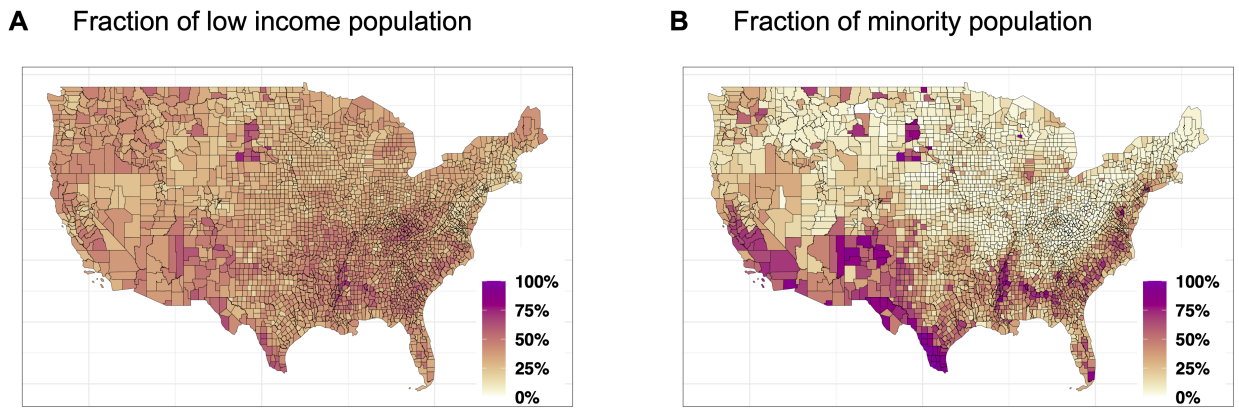

Figure S15: Percentage of low income and minority populations living in each county. Definitions of low income and minority groups are adopted from EPA's Environmental Justice Mapping and Screening Tool (EJSCREEN).

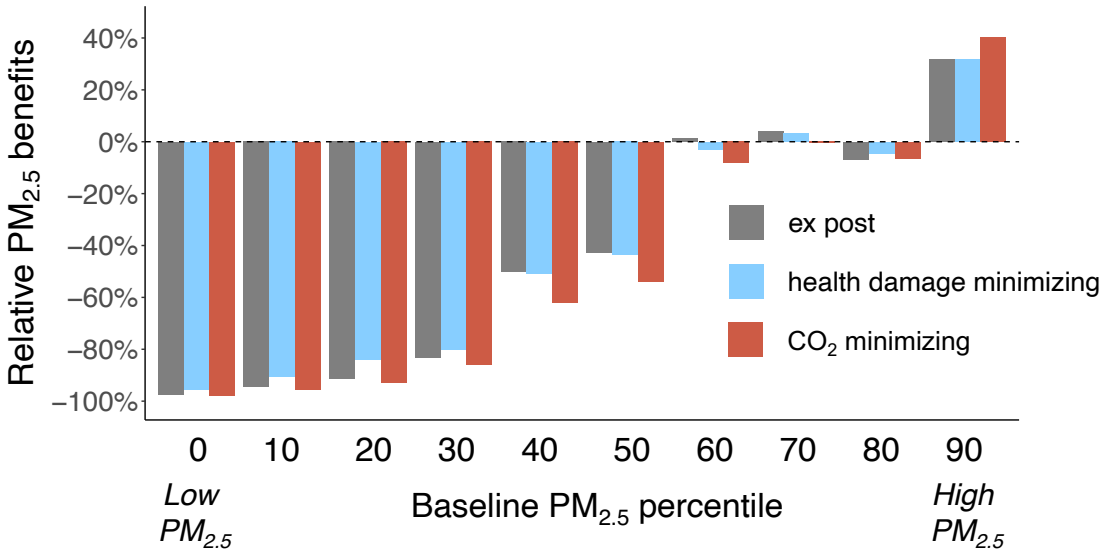

Figure S16: Percentage difference in air quality benefits for groups living in areas with different levels of $PM_{2.5}$ concentration. The x-axis shows the percentile of $PM_{2.5}$ concentration (from the cleanest areas (left) to the dirtiest areas (right)) of the studied regions. Positive relative benefits indicate the subgroup experiences a larger reduction in $PM_{2.5}$-related mortality rates compared to the average population in the studied regions. The three emissions scenarios are shown in different colors.

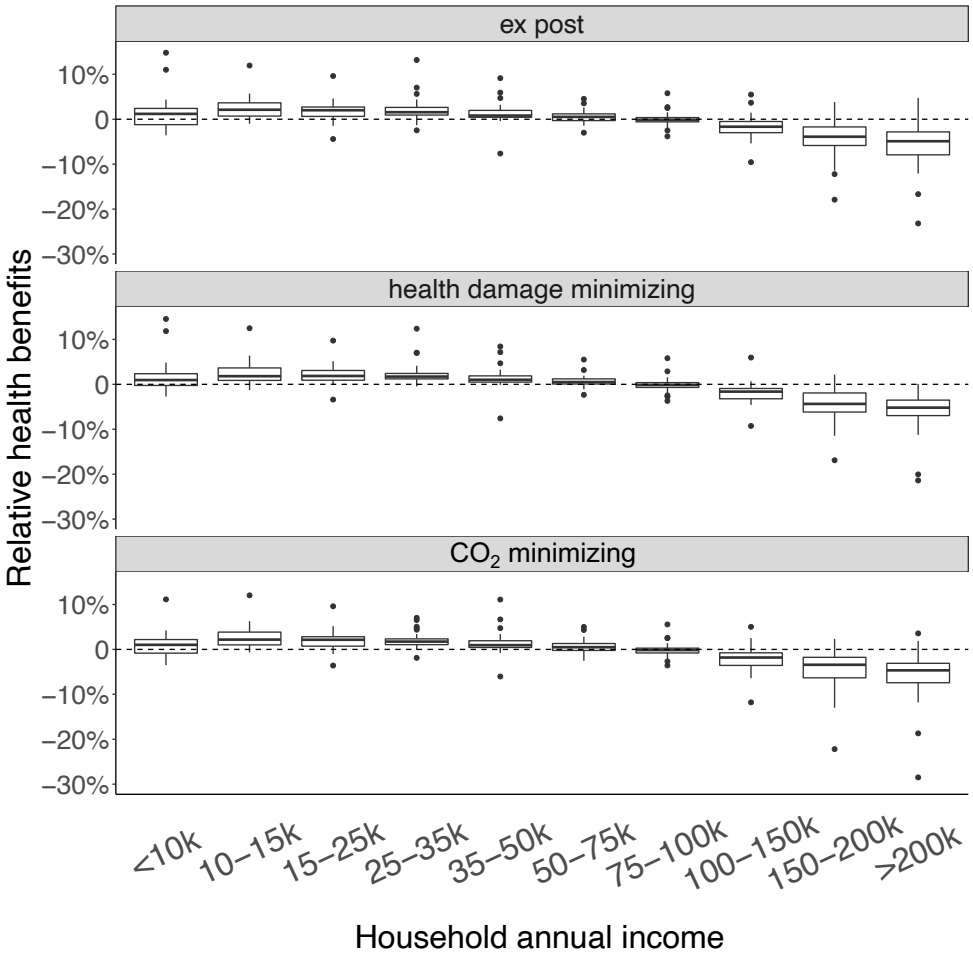

Figure S17: Percentage difference in air quality benefits for different income groups in each state. Each point on the box plot indicates a state. Positive relative benefits indicate the specific income group experiences a larger reduction in $PM_{2.5}$-related mortality rates compared with the state-wide average.

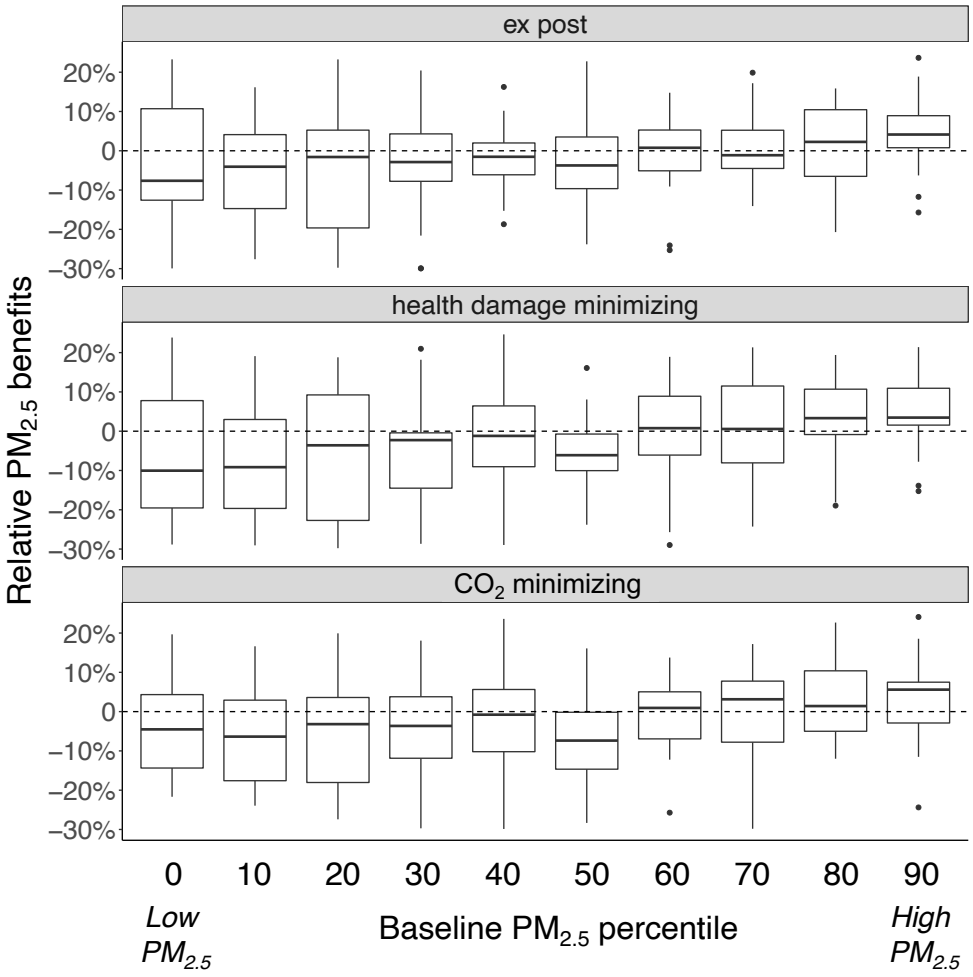

Figure S18: Percentage difference in air quality benefits for groups living in areas with different levels of $PM_{2.5}$ in each state. The x-axis shows the percentile of $PM_{2.5}$ concentration (from the cleanest areas (left) to the dirtiest areas (right)) in each state. Each point on the box plot indicates a state. Positive relative benefits indicate the specific population group experiences a larger reduction in $PM_{2.5}$-related mortality rates compared with the state-wide average.

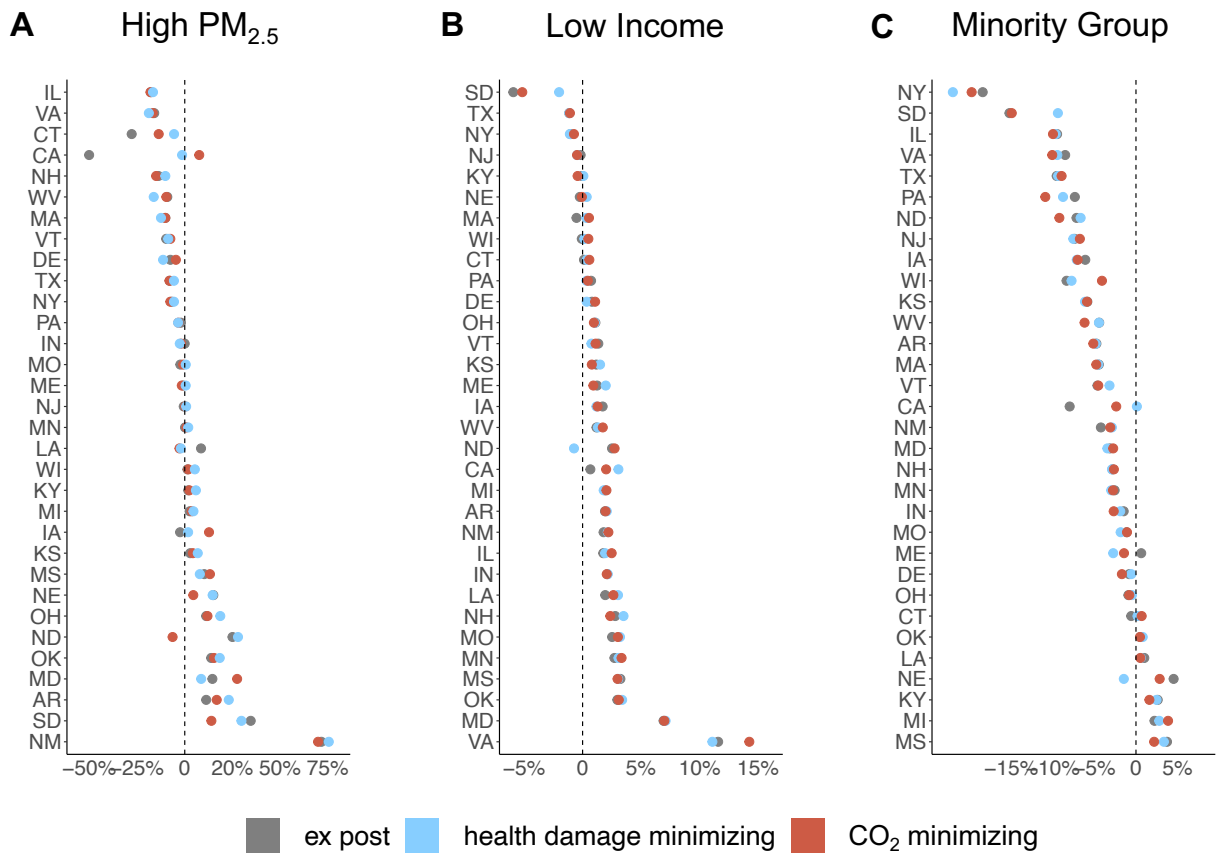

Figure S19: Relative $PM_{2.5}$ benefits within each state compared with the state-wide population. Positive relative benefits indicate the specific population group experiences a larger reduction in $PM_{2.5}$-related mortality rates compared to the state-wide average. Negative benefits indicate smaller reductions in mortality rates. The three emissions scenarios are shown in different colors.

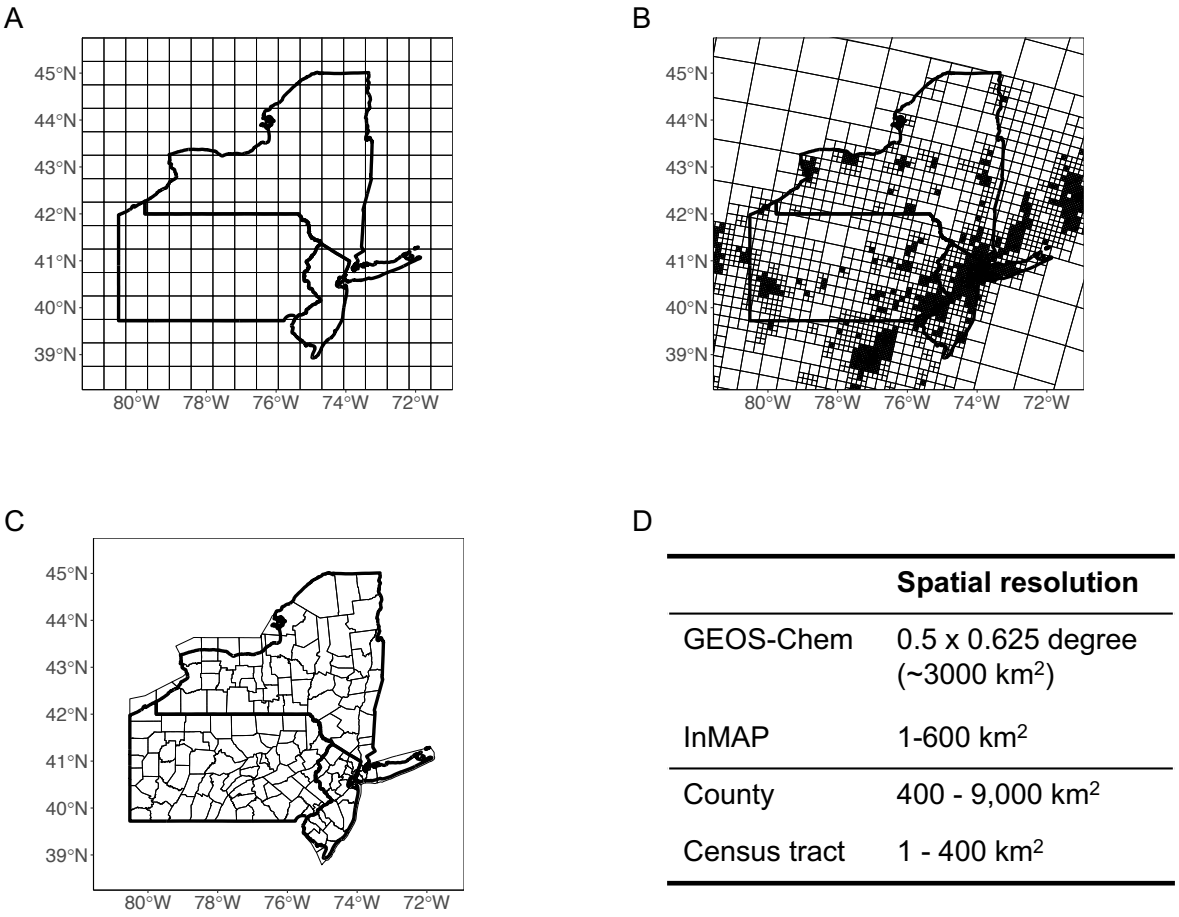

D

	Spatial resolution
GEOS-Chem	0.5 x 0.625 degree (~3000 km^2)
InMAP	1-600 km^2
County	400 - 9,000 km^2
Census tract	1 - 400 km^2

Figure S20: Spatial resolution of the GEOS-Chem model simulations (Panel A) and InMAP simulations (B). The size of GEOS-Chem grid cell is comparable to typical US counties (C). The grid cell size of InMAP varies dynamically based on the population density (smaller cell size in the urban populous regions). InMAP grid cell size is comparable to the size of census tracts (see table D). Table D shows the approximate size of GEOS-Chem grid cell, InMAP grid cell, county, and census tract. The 5th and 95th percentages of the spatial areas are shown for InMAP grid cells, US counties, and US census tracts.

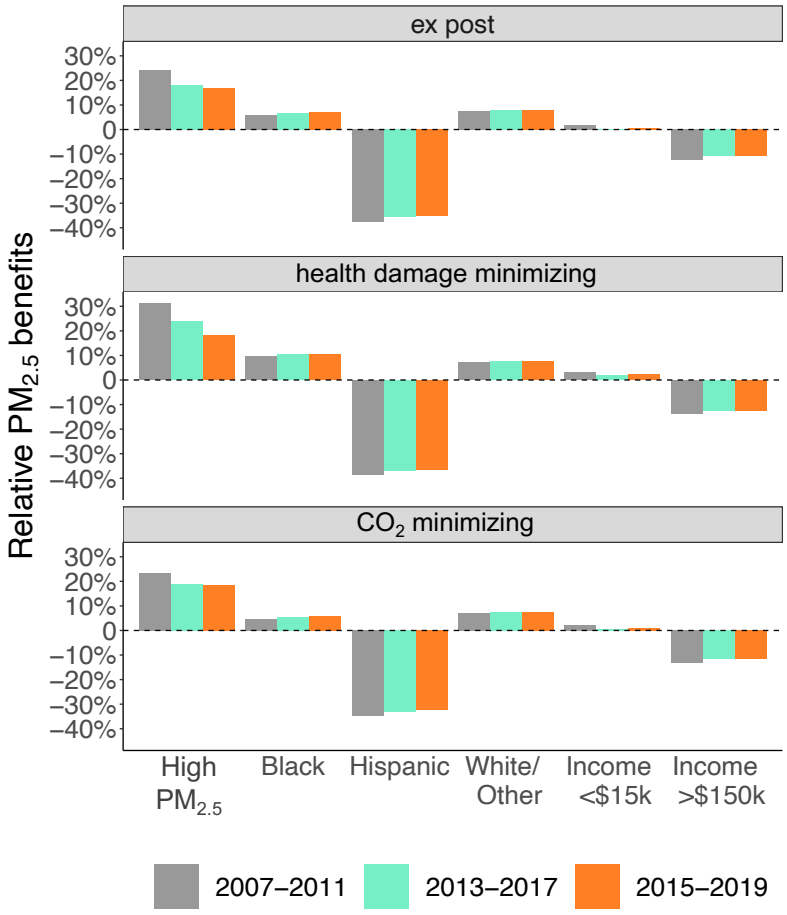

Figure S21: Percentage difference in air quality benefits for different demographic groups, calculated with demographic data of different years. Results are estimated with the American Community Survey (ACS) 5-year data from 2007-2011, 2013-2017, and 2015-2019, respectively. Benefits are calculated as the relative differences between the mortality rate changes experienced by specific population groups and the average population in the studied regions. The three panels show the result under three emissions scenarios.

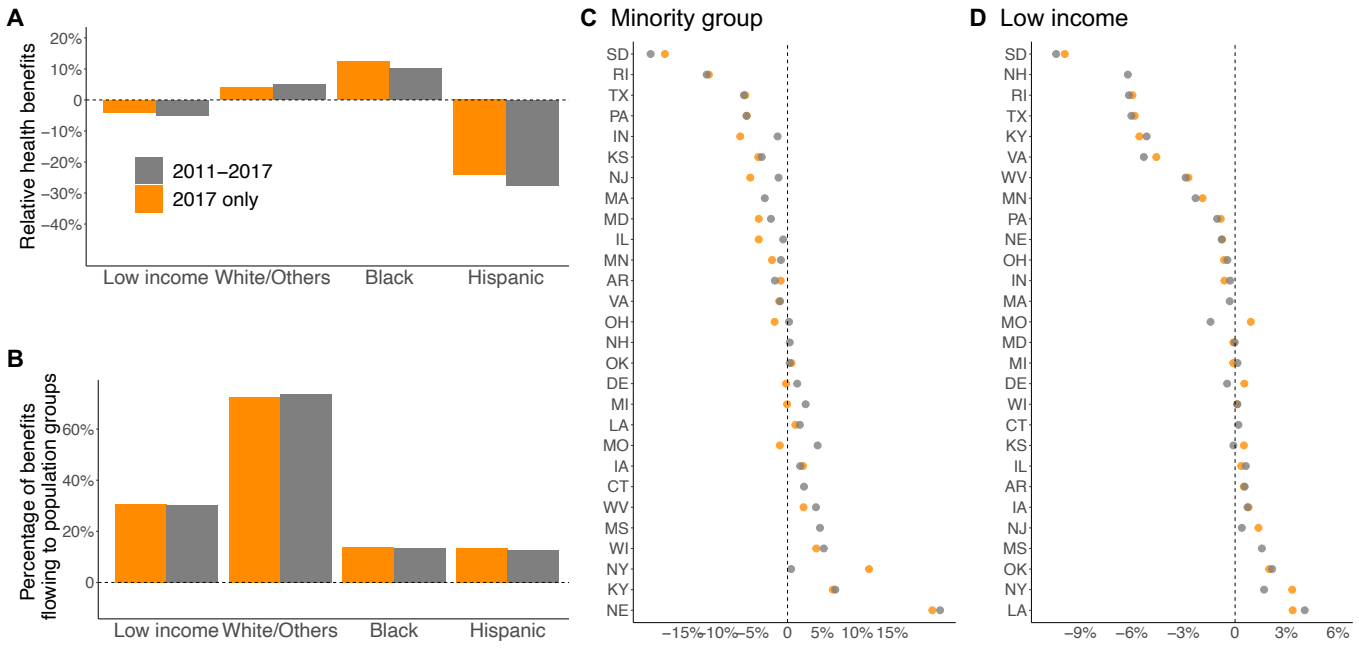

Figure S22: Distribution of air quality benefits for different racial and income groups, calculated with energy system data from 2011-2017 (main analysis) and data from 2017 alone. Panel A shows the relative differences between the mortality rate changes experienced by specific population groups and the average population in the studied regions. Panel B shows the faction of benefits accrued to each group. Panel C and D show the relative benefits at the state level. Results are estimated with the InMAP model.

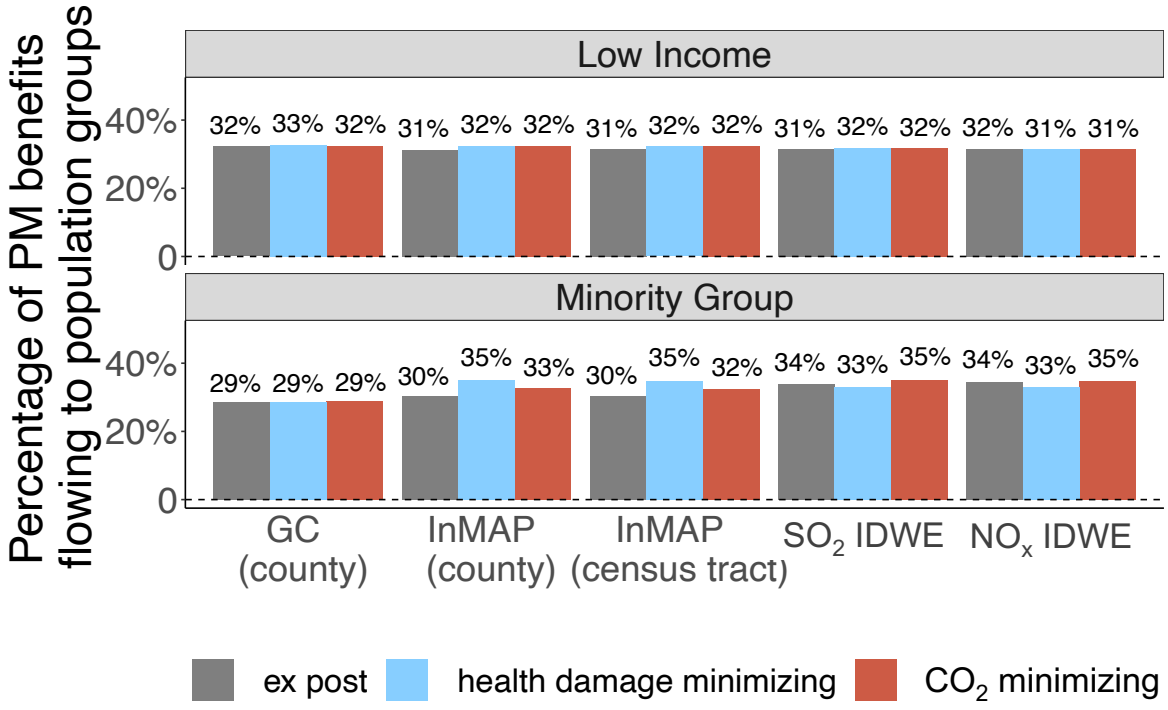

Figure S23: Percentage of total $PM_{2.5}$ benefits from wind power associated with RPS targets flowing to low income (upper panel) and minority populations (lower panel). Figure shows estimates derived from GEOS-Chem (GC (county)), InMAP at two different resolutions (at county and census tract level) and inverse distance weighted emissions (IDWE) using plant-level SO_2 and NO_x emissions. Avoided premature mortalities (health benefits) are calculated with county-specific mortality rates. Definitions of low income and minority groups are adopted from EPA's Environmental Justice Mapping and Screening Tool (EJSCREEN). The three emissions scenarios are shown in different colors.

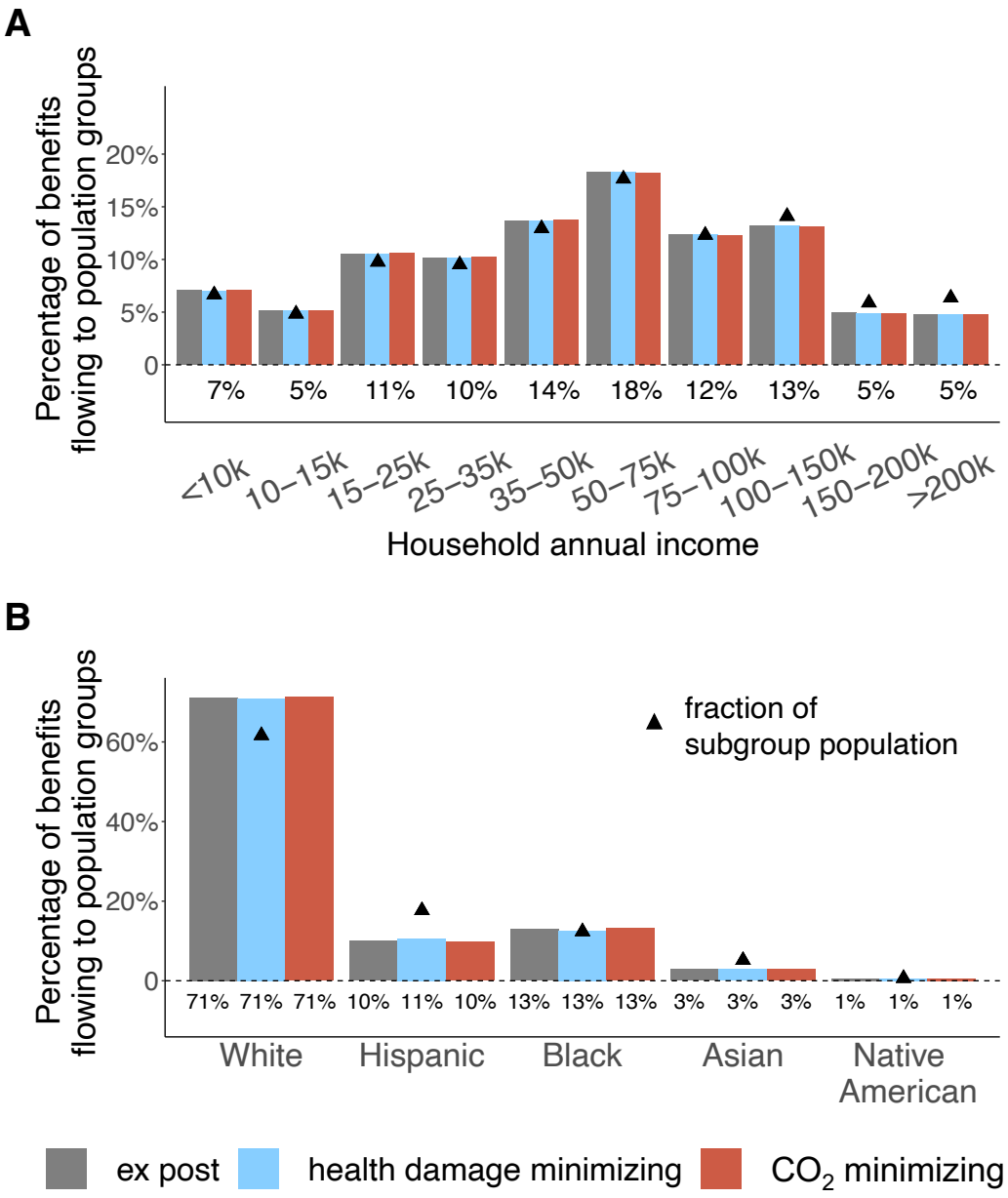

Figure S24: Percentage of total health benefits from wind power associated with RPS targets flowing to different income groups (upper panel) and racial/ethnic groups (lower panel). Black triangles show the population fraction of the subgroup. Figure shows estimates derived from GEOS-Chem. Health benefits are calculated with the avoided premature mortalities ($PM_{2.5}$ and O_3). The three emissions scenarios are shown in different colors.

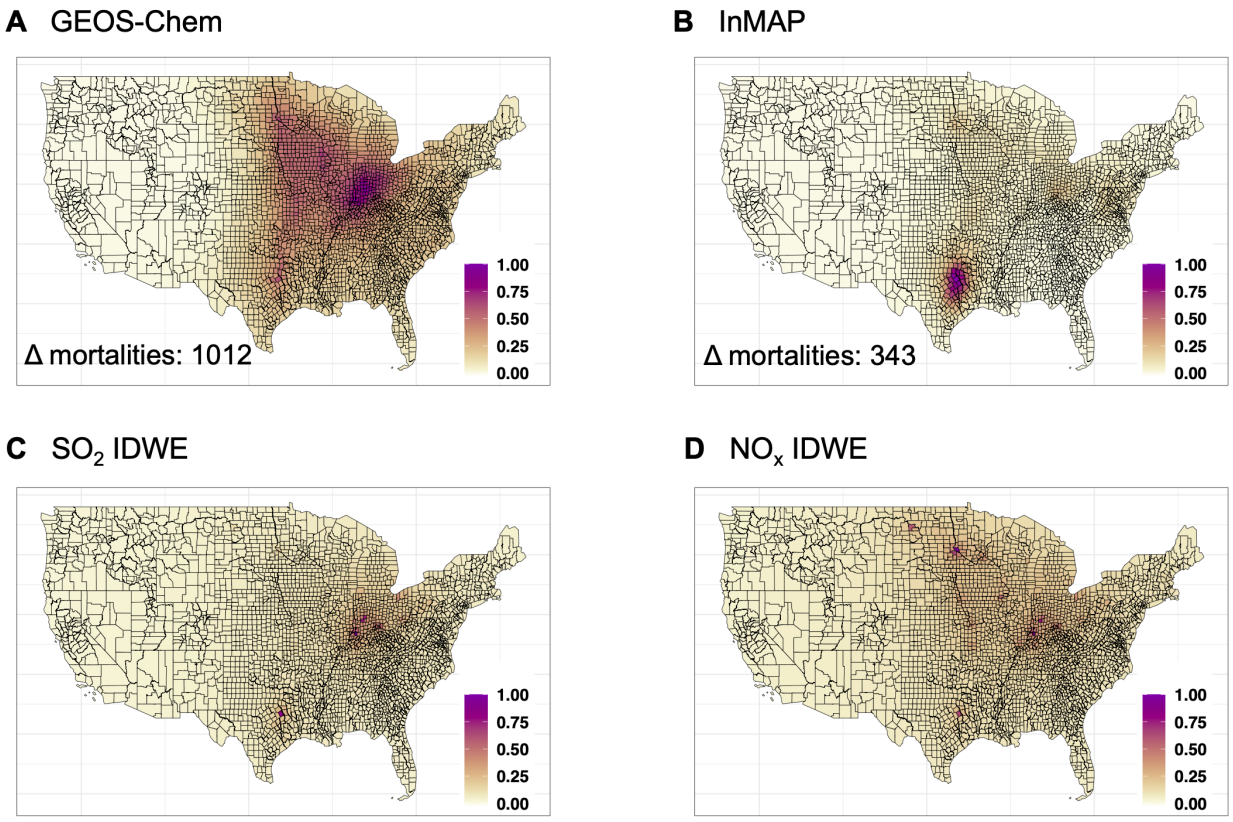

Figure S25: Normalized changes in pollution exposure of $PM_{2.5}$ under the health damage minimizing scenario using different air quality modeling approaches. The changes in the county-level exposure are normalized as the ratio to the largest change in the pollution exposure (i.e. the exposure is one in the county with the largest change in pollution exposure). The $PM_{2.5}$ exposure is modeled as concentrations (unit: $\mu g/m^3$) in GEOS-Chem and InMAP, and modeled as inverse distanced emissions in IDWE. The total number of avoided mortality under the health damage minimizing scenario is included for GEOS-Chem and InMAP estimates.

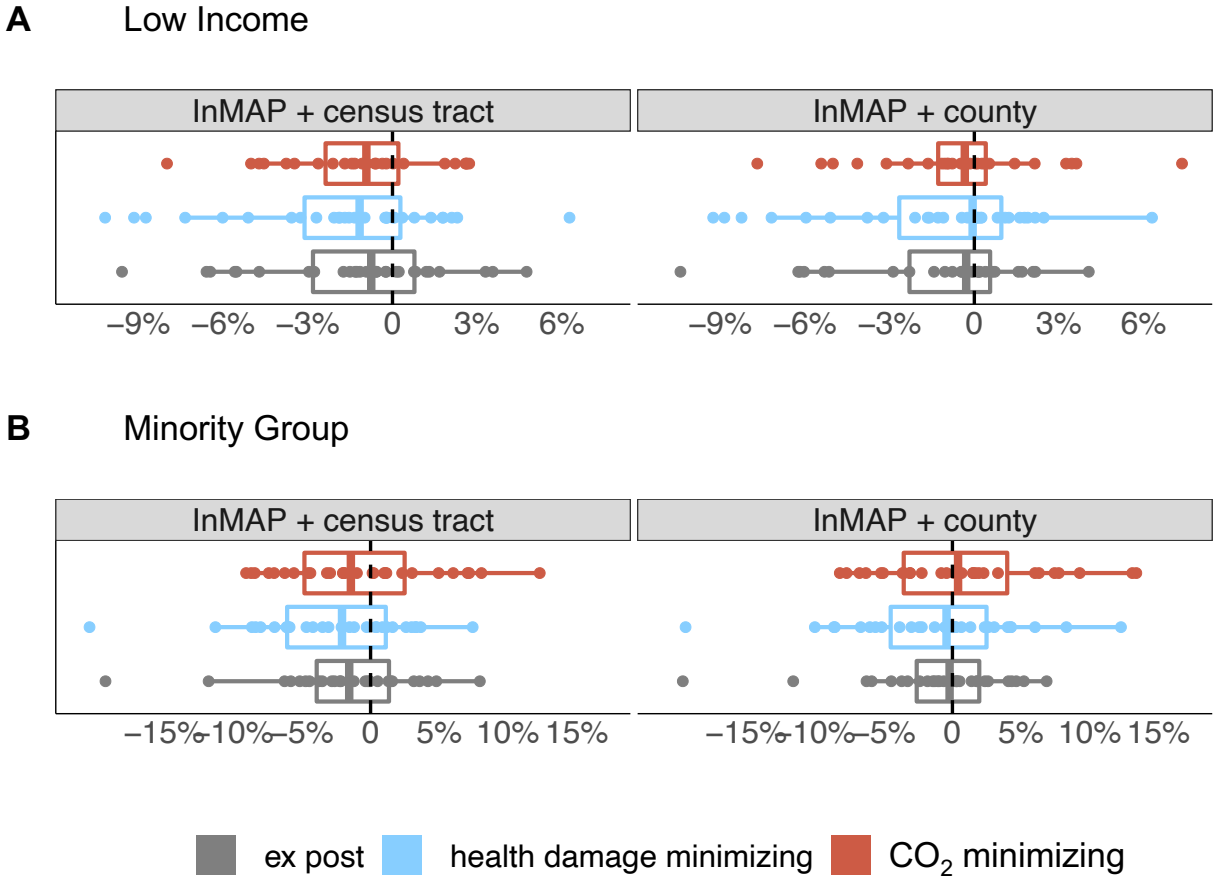

Figure S26: Relative $PM_{2.5}$ benefits for low income and minority groups within each state (estimated with InMAP). This figure shows the results calculated with InMAP at county and census tract level. Positive relative benefits indicate the specific population group experiences a larger reduction in $PM_{2.5}$-related mortality rates compared to the state-wide average. Negative benefits indicate smaller reductions in mortality rates. The three emissions scenarios are shown in different colors.

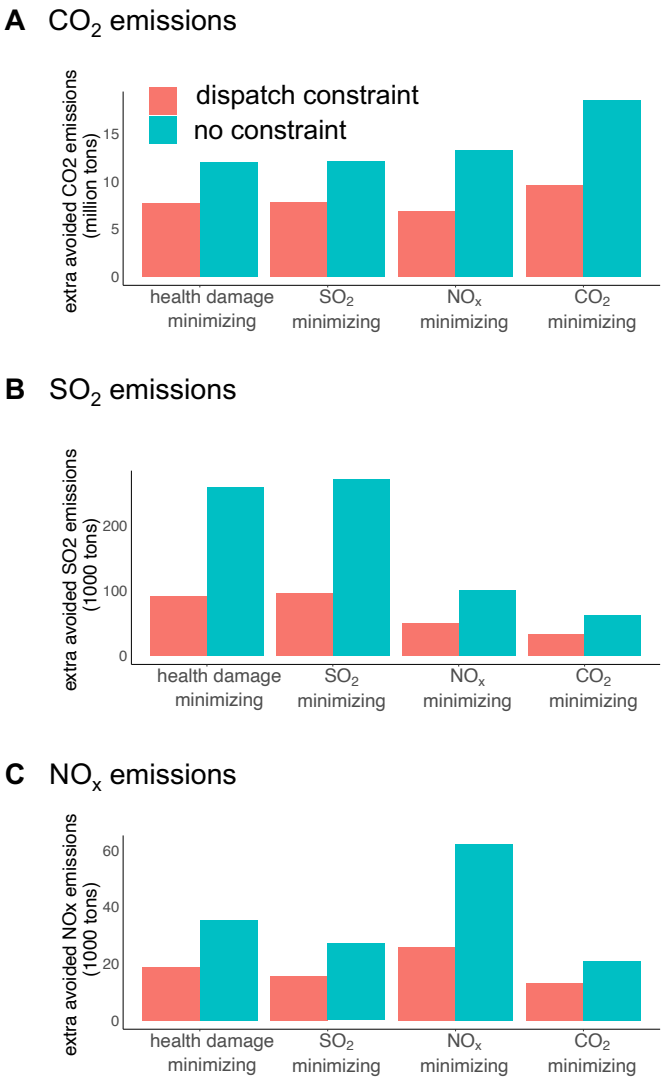

Figure S27: The extra avoided emissions under idealized theoretical scenarios with (red) and without dispatch constraints (turquoise) relative to the *ex post* scenario. Dispatch constraints are determined by the interannual variability of unit-level generation (ranging from 1%-30%), which are used to limit the fraction of electricity generation that can be displaced by wind power in any given hour.

REFERENCES AND NOTES

1. S. Carley, L. L. Davies, D. B. Spence, N. Zirogiannis, Empirical evaluation of the stringency and design of renewable portfolio standards. *Nat. Energy* **3**, 754–763 (2018).

2. H. Yin, N. Powers, Do state renewable portfolio standards promote in-state renewable generation? *Energy Policy* **38**, 1140–1149 (2010).

3. F. C. Menz, S. Vachon, The effectiveness of different policy regimes for promoting wind power: Experiences from the states. *Energy Policy* **34**, 1786–1796 (2006).

4. S. Carley, State renewable energy electricity policies: An empirical evaluation of effectiveness. *Energy Policy* **37**, 3071–3081 (2009).

5. G. Shrimali, G. Chan, S. Jenner, F. Groba, J. Indvik, Evaluating renewable portfolio standards for in-state renewable deployment: Accounting for policy heterogeneity. *Econ. Energy Environ. Policy* **4**, 127–142 (2015).

6. G. Shrimali, J. Kniefel, Are government policies effective in promoting deployment of renewable electricity resources? *Energy Policy* **39**, 4726–4741 (2011).

7. L. J. L. Eastin, An assessment of the effectiveness of renewable portfolio standards in the United States. *Electr. J.* **27**, 126–137 (2014).

8. J. Janak, Do renewable portfolio standards increase renewable energy capacity? Evidence from the United States. *J. Environ. Manage.* **287**, 112261 (2021).

9. W. Katzenstein, J. Apt, Air emissions due to wind and solar power. *Environ. Sci. Tech.* **43**, 253–258 (2009).

10. J. Cullen, Measuring the environmental benefits of wind-generated electricity. *Am. Econ. J. Econ. Policy* **5**, 107–133 (2013).

11. K. Novan, Valuing the wind: Renewable energy policies and air pollution avoided. *Am. Econ. J. Econ. Policy* **7**, 291–326 (2015).

12. H. Fell, J. X. Johnson, Regional disparities in emissions reduction and net trade from renewables. *Nat. Sustain.* **4**, 358–365 (2021).

13. K. Siler-Evans, I. L. Azevedo, M. G. Morgan, Marginal emissions factors for the U.S. electricity system. *Environ. Sci. Tech.* **46**, 4742–4748 (2012).

14. T. A. Deetjen, I. L. Azevedo, Reduced-order dispatch model for simulating marginal emissions factors for the United States power sector. *Environ. Sci. Tech.* **53**, 10506–10513 (2019).

15. D. Millstein, R. Wiser, M. Bolinger, G. Barbose, The climate and air-quality benefits of wind and solar power in the united states. *Nat. Energy* **2**, 17134 (2017).

16. K. Siler-Evans, I. L. Azevedo, M. G. Morgan, J. Apt, Regional variations in the health, environmental, and climate benefits of wind and solar generation. *Proc. Natl. Acad. Sci. U.S.A.* **110**, 11768–11773 (2013).

17. R. Wiser, M. Bolinger, G. Heath, D. Keyser, E. Lantz, J. Macknick, T. Mai, D. Millstein, Long-term implications of sustained wind power growth in the United States: Potential benefits and secondary impacts. *Appl. Energy* **179**, 146–158 (2016).

18. R. Wiser, T. Mai, D. Millstein, G. Barbose, L. Bird, J. Heeter, D. Keyser, V. Krishnan, J. Macknick, Assessing the costs and benefits of US renewable portfolio standards. *Environ. Res. Lett.* **12**, 094023 (2017).

19. E. G. Dimanchev, S. Paltsev, M. Yuan, D. Rothenberg, C. W. Tessum, J. D. Marshall, N. E. Selin, Health co-benefits of sub-national renewable energy policy in the US. *Environ. Res. Lett.* **14**, 085012 (2019).

20. B. J. Sergi, P. J. Adams, N. Z. Muller, A. L. Robinson, S. J. Davis, J. D. Marshall, I. L. Azevedo, Optimizing emissions reductions from the U.S. power sector for climate and health benefits. *Environ. Sci. Tech.* **54**, 7513–7523 (2020).

21. R. D. Bullard, Environmental justice: It's more than waste facility siting. *Soc. Sci. Q.* **77**, 493–499 (1996).

22. N. Z. Muller, P. H. Matthews, V. Wiltshire-Gordon, The distribution of income is worse than you think: Including pollution impacts into measures of income inequality. *PLOS ONE* **13**, e0192461 (2018).

23. C. W. Tessum, J. S. Apte, A. L. Goodkind, N. Z. Muller, K. A. Mullins, D. A. Paolella, S. Polasky, N. P. Springer, S. K. Thakrar, J. D. Marshall, J. D. Hill, Inequity in consumption of goods and services adds to racial–ethnic disparities in air pollution exposure. *Proc. Natl. Acad. Sci. U.S.A.* **116**, 6001–6006 (2019).

24. S. E. Chambliss, C. P. R. Pinon, K. P. Messier, B. LaFranchi, C. R. Upperman, M. M. Lunden, A. L. Robinson, J. D. Marshall, J. S. Apte, Local- and regional-scale racial and ethnic disparities in air pollution determined by long-term mobile monitoring. *Proc. Natl. Acad. Sci. U.S.A.* **118**, e2109249118 (2021).

25. J. Liu, L. P. Clark, M. J. Bechle, A. Hajat, S.Y. Kim, A. L. Robinson, L. Sheppard, A. A. Szpiro, J. D. Marshall, Disparities in air pollution exposure in the united states by race/ethnicity and income, 1990–2010. *Environ. Health Perspect.* **129**, 127005 (2021).

26. A. Jbaily, X. Zhou, J. Liu, T.-H. Lee, L. Kamareddine, S. Verguet, F. Dominici, Air pollution exposure disparities across US population and income groups. *Nature* **601**, 228–233 (2022).

27. C. W. Tessum, D. A. Paolella, S. E. Chambliss, J. S. Apte, J. D. Hill, J. D. Marshall, $PM_{2.5}$ polluters disproportionately and systemically affect people of color in the United States. *Sci. Adv.* **7**, eabf4491 (2021).

28. H. M. Lane, R. Morello-Frosch, J. D. Marshall, J. S. Apte, Historical redlining is associated with present-day air pollution disparities in U.S. cities. *Environ. Sci. Technol. Lett.* **9**, 345–350 (2022).

29. R. Gardner-Frolick, D. Boyd, A. Giang, Selecting data analytic and modeling methods to support air pollution and environmental justice investigations: A critical review and guidance framework. *Environ. Sci. Technol.* **56**, 2843–2860 (2022).

30. The White House, “Executive order on tackling the climate crisis at home and abroad” (NEPA Policy and Compliance, 2021).

31. T. M. Thompson, S. Rausch, R. K. Saari, N. E. Selin, A systems approach to evaluating the air quality co-benefits of US carbon policies. *Nat. Clim. Chang.* **4**, 917–923 (2014).

32. G. Barbose, R. Wiser, J. Heeter, T. Mai, L. Bird, M. Bolinger, A. Carpenter, G. Heath, D. Keyser, J. Macknick, A. Mills, D. Millstein, A retrospective analysis of benefits and impacts of U.S. renewable portfolio standards. *Energy Policy* **96**, 645–660 (2016).

33. S. Zhu, M. Mac Kinnon, A. Carlos-Carlos, S. J. Davis, S. Samuelsen, Decarbonization will lead to more equitable air quality in California. *Nat. Commun.* **13**, 5738 (2022).

34. C. M. Anderson, K. A. Kissel, C. B. Field, K. J. Mach, Climate change mitigation, air pollution, and environmental justice in California. *Environ. Sci. Tech.* **52**, 10829–10838 (2018).

35. C. Grainger, T. Ruangmas, Who wins from emissions trading? Evidence from California. *Environ. Resource Econ.* **71**, 703–727 (2018).

36. S. P. Holland, E. T. Mansur, N. Z. Muller, A. J. Yates, Distributional effects of air pollution from electric vehicle adoption. *J. Assoc. Environ. Resour. Econ.* **6**, S65–S94 (2019).

37. D. Hernandez-Cortes, K. C. Meng, “Do environmental markets cause environmental injustice? Evidence from California’s carbon market” (Technical Report, National Bureau of Economic Research, 2020).

38. I. C. Dedoussi, S. D. Eastham, E. Monier, S. R. H. Barrett, Premature mortality related to United States cross-state air pollution. *Nature* **578**, 261–265 (2020).

39. U.S. Energy Information Administration, “Hourly electric grid monitor (2018–2021)” (EIA, 2021).

40. H. Fell, D. T. Kaffine, The fall of coal: Joint impacts of fuel prices and renewables on generation and emissions. *Am. Econ. J. Econ. Policy* **10**, 90–116 (2018).

41. H. Fell, D. T. Kaffine, K. Novan, Emissions, transmission, and the environmental value of renewable energy. *Am. Econ. J. Econ. Policy* **13**, 241–272 (2021).

42. D. Krewski, M. Jerrett, R. T. Burnett, R. Ma, E. Hughes, Y. Shi, M. C. Turner, C. A. Pope III, G. Thurston, E. E. Calle, M. J. Thun, B. Beckerman, P. De Luca, N. Finkelstein, K. Ito, D. K. Moore, K. B. Newbold, T. Ramsay, Z. Ross, H. Shin, B. Tempalski, Extended follow-up and spatial analysis of the American Cancer Society study linking particulate air pollution and mortality. *Res. Rep. Health Eff. Inst.* **140**, 5–114 (2009).

43. M. C. Turner, M. Jerrett, C. A. Pope III, D. Krewski, S. M. Gapstur, W. R. Diver, B. S. Beckerman, J. D. Marshall, J. Su, D. L. Crouse, R. T. Burnett, Long-term ozone exposure and mortality in a large prospective study. *Am. J. Respir. Crit. Care Med.* **193**, 1134–1142 (2016).

44. National Center for Environmental Economics, "Guidelines for preparing economic analyses" (EPA, 2014); www.epa.gov/environmental-economics/guidelines-preparing-economic-analyses.

45. L. Valentino, V. Valenzuela, A. Botterud, Z. Zhou, G. Conzelmann, System-wide emissions implications of increased wind power penetration. *Environ. Sci. Tech.* **46**, 4200–4206 (2012).

46. E. Denny, M. O'Malley, Wind generation, power system operation, and emissions reduction. *IEEE Trans. Power Syst.* **21**, 341–347 (2006).

47. Interagency Working Group on Social Cost of Greenhouse Gases, United States Government, "Technical support document: Technical update of the social cost of carbon for regulatory impact analysis under executive order 12866" (Technical Report, 2016).

48. J. J. Buonocore, E. J. Hughes, D. R. Michanowicz, J. Heo, J. G. Allen, A. Williams, Climate and health benefits of increasing renewable energy deployment in the United States. *Environ. Res. Lett.* **14**, 114010 (2019).

49. T. Stehly, P. Beiter, D. Heimiller, G. Scott, "2017 Cost of wind energy review" (National Renewable Energy Laboratory, 2018).

50. U.S. Environmental Protection Agency, “EJScreen: Environmental justice screening and mapping tool: Technical documentation for EJScreen” (EPA, 2019); www.epa.gov/sites/default/files/2021-04/documents/ejscreen_technical_document.pdf.

51. L. R. Henneman, I. C. Dedoussi, J. A. Casey, C. Choirat, S. R. H. Barrett, C. M. Zigler, Comparisons of simple and complex methods for quantifying exposure to individual point source air pollution emissions. *J. Expo. Sci. Environ. Epidemiol.* **31**, 654–663 (2021).

52. L. P. Clark, M. H. Harris, J. S. Apte, J. D. Marshall, National and intraurban air pollution exposure disparity estimates in the United States: Impact of data-aggregation spatial scale. *Environ. Sci. Technol. Lett.* **9**, 786–791 (2022).

53. T. P. Lyon, H. Yin, Why do states adopt renewable portfolio standards? An empirical investigation. *Energy J.* **31**, 133–157 (2010).

54. U.S. Environmental Protection Agency, “Air markets program data (CAMPD)” (CAMPD, 2021); https://campd.epa.gov/.

55. U.S. Environmental Protection Agency, “Emissions and generation resource integrated database (eGRID) 2014” (EPA, 2014); www.epa.gov/egrid.

56. U.S. Energy Information Administration, “Monthly and annual data on generation and fuel consumption at the power plant and prime mover level” (EIA-923 Reports) (EIA, 2021).

57. W. K. Newey, K. D. West, Automatic lag selection in covariance matrix estimation. *Rev. Econ Stud.* **61**, 631–653 (1994).

58. Y. Benjamini, Y. Hochberg, Controlling the false discovery rate: A practical and powerful approach to multiple testing. *J. R. Stat. Soc. B. Methodol.* **57**, 289–300 (1995).

59. I. Bey, D. J. Jacob, R. M. Yantosca, J. A. Logan, B. D. Field, A. M. Fiore, Q. Li, H. Y. Liu, L. J. Mickley, M. G. Schultz, Global modeling of tropospheric chemistry with assimilated meteorology: Model description and evaluation. *J. Geophys. Res. Atmos.* **106**, 23073–23095 (2001).

60. D. K. Henze, A. Hakami, J. H. Seinfeld, Development of the adjoint of GEOS-Chem. *Atmospheric Chem. Phys.* **7**, 2413–2433 (2007).

61. Y. X. Wang, M. B. McElroy, D. J. Jacob, R. M. Yantosca, A nested grid formulation for chemical transport over Asia: Applications to CO. *J. Geophys. Res. Atmos.* **109**, D22307 (2004).

62. J. Lepeule, F. Laden, D. Dockery, J. Schwartz, Chronic exposure to fine particles and mortality: An extended follow-up of the harvard six cities study from 1974 to 2009. *Environ. Health Perspect.* **120**, 965–970 (2012).

63. G. Hoek, R. M. Krishnan, R. Beelen, A. Peters, B. Ostro, B. Brunekreef, J. D. Kaufman, Long-term air pollution exposure and cardio-respiratory mortality: A review. *Environ. Health* **12**, 43 (2013).

64. Q. Di, Y. Wang, A. Zanobetti, Y. Wang, P. Koutrakis, C. Choirat, F. Dominici, J. D. Schwartz, Air pollution and mortality in the medicare population. *N. Engl. J. Med.* **376**, 2513–2522 (2017).

65. C. A. Pope III, M. Ezzati, J. B. Cannon, R. T. Allen, M. Jerrett, R. T. Burnett, Mortality risk and $PM_{2.5}$ air pollution in the USA: An analysis of a national prospective cohort. *Air Qual. Atmos. Health* **11**, 245–252 (2018).

66. World Health Organization, “WHO Mortality Database ICD-10” (WHO, 2019); www.who.int/data/data-collection-tools/who-mortality-database.

67. United States Department of Health and Human Services (US DHHS), Centers for Disease Control and Prevention (CDC), National Center for Health Statistics (NCHS), “Compressed Mortality File (CMF) on CDC WONDER Online Database” (U.S. Department of Health & Human Services, 2021).

68. Center for International Earth Science Information Network, Columbia University, “Gridded Population of the World, Version 4 (GPWv4): Population Count, Revision 11” (AquaKnow, 2018).

69. U.S. Census Bureau, “U.S. population by age and sex (2014 ACS 1-Year Estimates)” (United States Census Bureau, 2014).

70. U.S. Census Bureau, U.S. “Population by income, race and hispanic origins (ACS 5-Year Estimates, 2013–2017)” (United States Census Bureau, 2017).

71. M. S. Hammer, A. van Donkelaar, C. Li, A. Lyapustin, A. M. Sayer, N. C. Hsu, R. C. Levy, M. J. Garay, O. V. Kalashnikova, R. A. Kahn, M. Brauer, J. S. Apte, D. K. Henze, L. Zhang, Q. Zhang, B. Ford, J. R. Pierce, R. V. Martin, Global estimates and long-term trends of fine particulate matter concentrations (1998–2018). *Environ. Sci. Tech.* **54**, 7879–7890 (2020).

72. C. W. Tessum, J. D. Hill, J. D. Marshall, Inmap: A model for air pollution interventions. *PLOS ONE* **12**, e0176131 (2017).

73. Berkeley Lab Electricity Markets and Policy Group, “RPS compliance data and RPS percentage targets” (Berkeley Lab, 2021).

74. U.S. Department of Energy, “The 2020 national electric transmission congestion study” (Office of Electricity, 2020).

75. J. Colmer, I. Hardman, J. Shimshack, J. Voorheis, Disparities in $PM_{2.5}$ air pollution in the united states. *Science* **369**, 575–578 (2020).

76. N. Z. Muller, Linking policy to statistical uncertainty in air pollution damages. *B.E. J. Econ. Anal. Policy* **11**, 2925 (2011).

77. J. Heo, P. J. Adams, H. O. Gao, Reduced-form modeling of public health impacts of inorganic $PM_{2.5}$ and precursor emissions. *Atmos. Environ.* **137**, 80–89 (2016).

78. U.S. Environmental Protection Agency, “Regulatory impact analysis for the clean power plan final rule” (EPA, 2015).

79. R. Gelaro, W. McCarty, M. J. Suárez, R. Todling, A. Molod, L. Takacs, C. A. Randles, A. Darmenov, M. G. Bosilovich, R. Reichle, K. Wargan, L. Coy, R. Cullather, C. Draper, S. Akella,

V. Buchard, A. Conaty, A. M. da Silva, W. Gu, G.K. Kim, R. Koster, R. Lucchesi, D. Merkova, J. E. Nielsen, G. Partyka, S. Pawson, W. Putman, M. Rienecker, S. D. Schubert, M. Sienkiewicz, B. Zhao, The modern-era retrospective analysis for research and applications, version 2 (MERRA-2). *J. Climate* **30**, 5419–5454 (2017).

80. S. E. Sexton, A. J. Kirkpatrick, R. Harris, N. Z. Muller, "Heterogeneous environmental and grid benefits from rooftop solar and the costs of inefficient siting decisions" (Technical Report, National Bureau of Economic Research, 2018).